Printed in U.S.A.

Paper No.
75-DET-116

an ASME publication

$3.00 PER COPY $1.00 TO ASME MEMBERS

R. G. Kirk
Senior Analyst,
Ingersoll Rand Company,
Phillipsburg, N. J. Assoc. Mem. ASME

E. J. Gunter
Professor,
Dept. of Mechanical Engineering,
University of Virginia,
Charlottesville, Va. Mem. ASME

Stability and Transient Motion of a Plain Journal Mounted in Flexible Damped Supports

This paper treats the effect of support damping and flexibility on the response characteristics of a symmetric rotor mounted in journal bearings. The successful operation of turbomachinery utilizing fluid-film bearings is shown to be very dependent upon the bearing support structure for high-speed applications. A stability analysis is discussed based upon the application of both the Routh criteria and the calculation of damped eigenvalues. Results are plotted for typical rotor support properties. The analysis also discusses the influence of rotor imbalance on the stability of rotor systems, and time transient orbits of shaft and support motions clearly indicate their dynamic behavior for both the stable and unstable operating speeds. Simplified design criteria are given for the selection of the support stiffness and damping based upon rotor weight and journal clearance to promote optimum stability. The stability analysis shows that the stability threshold with a damper support may increase the stability level over four times the value of a journal bearing on a rigid support. A nonlinear transient analysis is presented to show the size the journal limit cycles and forces transmitted with and without a damper support.

1 Introduction

The dynamics of rotor bearing systems has become of extreme importance due to the increased speed and power level requirements of advanced design rotating equipment. The aircraft jet engine industry has as their ultimate goal a lighter, more powerful, more efficient, and more dependable power plant. Compressor and industrial gas turbine manufacturers are concerned with reduced development costs, high reliability, and low maintenance costs over extended useful service life. These factors are responsible for the interest in and growth of the study of stability and forced response of rotor bearing systems. Power plants for ground installation and outer space are relying on fluid-film bearing to provide long, maintenance free service. To avoid the classical instability associated with plain cylindrical bearings the designers have used multi-lobe, tilting pad, pressure dam, and other designs such as herringbone groove to increase the stable speed range of their equipment.

Jet engine manufacturers are designing advanced engines with anti-friction bearings in series with fluid-film dampers to reduce engine sensitivity to imbalance. In qualitative terms, the same system parameters which promote optimum forced response characteristics are also conductive to an increased stable operating speed range. While this is true in general, it is extremely important for the dynamist to fully understand the cause and nature of instabilities associated with fluid-film bearings, internal friction damping, and aerodynamic cross-coupling. The present paper will be concerned with only those instabilities associated with fluid-film bearings. The instability associated with the plain cylindrical journal bearing has received considerable attention in the literature [1–5]. Pinkus [6] reported that flexible mountings gave greater stability to rotor bearing systems while Poritsky [7] and Hagg and Warner

Contributed by the Design Engineering Division for presentation at the Design Engineering Technical Conference, Washington, D.C., September 17–19, 1975 of THE AMERICAN SOCIETY OF MECHANICAL ENGINEERS. Manuscript received at ASME Headquarters June 10, 1975. Paper No. 75-DET-116.
Copies will be available until June, 1976

[1] Numbers in brackets designate References at end of paper.

[8] found that support flexibility lowered the stability threshold speed. Gunter [9] explained the discrepancy when it was shown that a symmetrical undamped support lowered the threshold speed whereas damped and/or asymmetric supports can greatly increase the stability of a rotor system.

Hori [10] presented an analysis of a long bearing with negative fluid film pressures neglected (to model cavitation) which indicated that the journal was not inherently unstable at all speeds as Robertson [3] had shown. Hori's analysis was in agreement with practical experience and all future investigations have included the cavitation effects unless supply pressures are in excess of the peak film pressures in which case the film does not cavitate. Hori concluded that the vertical balanced journal would be unstable at all speeds. This fact has been demonstrated by the authors, and it has been determined that rotor imbalance is required to promote stability of vertical rotors operating in plain journal bearings [22].

An investigation by Badgley [11] reported on a time transient analysis method of obtaining the stability threshold speed of short, long and finite bearings. The orbits of a balanced horizontal rotor on rigid supports were examined for various methods of pertubation to determine the influence on the stability boundary. He indicated that the threshold speed at high eccentricities is reduced by large initial velocities. (The results obtained for the short bearings are shown in Fig. 5 of this paper). Lund [12] examined the stability of a flexible rotor with damped supports and concluded that damped flexible supports can considerably increase the threshold speed. Stability curves for specific rotor systems were presented for rotors supported in cylindrical gas bearings. Gunter [13] presented a linear analysis of the influence of damped supports on the response characteristics of a rigid rotor including gyroscopic effects. The analysis of a typical rotor system indicated significant reductions of forces transmitted for damped bearing supports.

Recent investigations of rotor stability [14, 15] have extended the rotor models to general multi-mass flexible rotors with damped bearings. These analyses are generally intended to study complex rotor systems and will add enormous capability to the rotor dynamist in future studies of stability.

The purpose of the following discussion is to present the results of an extensive study of the influence of damped flexible supports on the stability threshold speed of a rotor in nonlinear fluid film bearings [16, 17]. Stability maps are presented in dimensionless form for a range of support stiffness, damping, and mass ratios. Numerous time transient response orbits will indicate the nature of stable and unstable response orbits for both balanced and unbalanced rotor systems. Examination of the complex eigenvalues for a specific rotor system will give further insight to explain why rotors may pass through an unstable speed range and restabilize, only to go unstable at some higher speed in the classical "half-frequency whirl."

When shaft flexibility is included in the analysis another possible mode of instability is introduced which corresponds to the condition of "resonant whip" as reported by Newkirk [18]. This phenomena can be shown analytically by examination of damped eigenvalues. The examination of the real part of the eigenvalue gives not only an indication of whether the system is stable or unstable, but also an accurate indication of the rate of growth of small pertubations. This additional information has proven to be extremely useful in giving added insight to the cause and nature of rotor-bearing instability.

2 Description of Rotor Bearing System

2.1 Rotor and Support System. The system that is to be considered in this analysis is the symmetrical rotor as shown in Fig. 1. The rotor is considered to be supported by nonlinear fluid film bearings in which the length to diameter ratio is less than one (i.e., $L/D < 1.0$). The bearings are modeled by the short bearing approximation [19, 22]. A derivation of the fluid-film forces expressed in fixed cartesian coordinates is presented in the following

Nomenclature

a = growth factor (T^{-1})
c = journal bearing radial clearance (L)
C_{xx}, C_{yy} = bearing direct damping (FTL^{-1})
C_{xy}, C_{yx} = bearing cross coupled damping (FTL^{-1})
C_{1xx}, C_{1yy} = support direct damping (FTL^{-1})
C_{1xy}, C_{1yx} = support cross coupled damping (FTL^{-1})
$\bar{C}_B$ = support damping $(DIM.)$
D = journal bearing diameter (L)
e_μ = imbalance of rotor/m (L)
E_μ = imbalance ratio, $= e_\mu/c$ $(DIM.)$
F_x, F_y = journal fluid-film force (F)
g = gravitational constant (LT^{-2})
h = film thickness (L)
H = film thickness ratio, $= h/c$ $(DIM.)$
$\bar{K}_B$ = support stiffness $(DIM.)$
K_S = shaft stiffness (FL^{-1})
K_{xx}, K_{yy} = bearing direct stiffness (FL^{-1})
K_{xy}, K_{yx} = bearing cross coupled stiffness (FL^{-1})
K_{1xx}, K_{1yy} = support direct stiffness (FL^{-1})
K_{1xy}, K_{1yx} = support cross coupled stiffness (FL^{-1})
L = journal bearing length (L)
m_2 = rotor mass (FT^2L^{-1})
m_1 = support mass (FT^2L^{-1})
m = one-half equivalent rotor mass, $m_j + m_2/2$ (FT^2L^{-1})
m_j = journal bearing mass (FT^2L^{-1})
δ_m = mass ratio, $= m_1/m$ $(DIM.)$
N = rotor spin, $\omega/2\pi$ (REV/T)
R = journal radius (L)
S = Sommerfeld number $(REV.)$
S_s = Ocvirk number, $= S(L/D)^2$ $(REV.)$
w = parameter $= \mu RL^3\omega/2c^2$ (FL^{-2})
W = bearing loading (F)
$\bar{W}$ = load number $\equiv 2\pi W/\mu LD(2c/L)^2\sqrt{mc/W}$ $(REV.^{-1})$
x_1, y_1 = support displacement (L)
x_2, y_2 = rotor absolute displacement (L)
x_j, y_j = journal relative motion (L)
X, Y = displacement ratio, $= x/c$, y/c $(DIM.)$
X_0, Y_0 = journal equilibrium position $(DIM.)$
ϵ = journal eccentricity ratio $(DIM.)$
ϵ_0 = journal equilibrium eccentricity $(DIM.)$
λ = complex eigenvalue (T^{-1})
μ = viscosity of lubricant (FTL^{-2})
ϕ = attitude angle (rad)
ω_b = bearing spin rate (T^{-1})
ω_j = rotor spin rate (T^{-1})
ω = sum of $\omega_j + \omega_b$ (T^{-1})
ω_s = stability parameter, $= \omega\sqrt{mc/W}$ $(DIM.)$
Ω = whirl rate ratio, $= \dot{\phi}/\omega_j$ $(DIM.)$
CL = journal clearance (L)
CBX, CBY = support damping (FTL^{-1})
EMU = journal eccentricity ratio, $\equiv E_\mu$ $(DIM.)$
ES = journal equilibrium eccentricity ratio, $\equiv \epsilon_0$ $(DIM.)$
ESU = ϵ_0 calculated for LOAD = FU $(DIM.)$
FO = rotating load (F)
$FMAX$ = maximum fluid-film force (F)
$FMAXB$ = maximum force to bearing (F)
$FMAXS$ = maximum force to support (F)
FU = imbalance load (F)
$FURATIO$ = imbalance ratio, FU/W $(DIM.)$
$MU@5$ = viscosity of lubricant $(\times 10^5)$ (FTL^{-2})
SS = Ocvirk number $(REV.)$
$TRDMAX$ = maximum dynamic load/me $\mu\omega_j^2$ $(DIM.)$
$TRSMAX$ = maximum film load/W $(DIM.)$
W = bearing load from rotor (F)
WB = bearing weight (F)
WJ = journal weight (F)
WS = stability parameter, ω_s $(DIM.)$
WT = (total load on bearing)/W $(DIM.)$

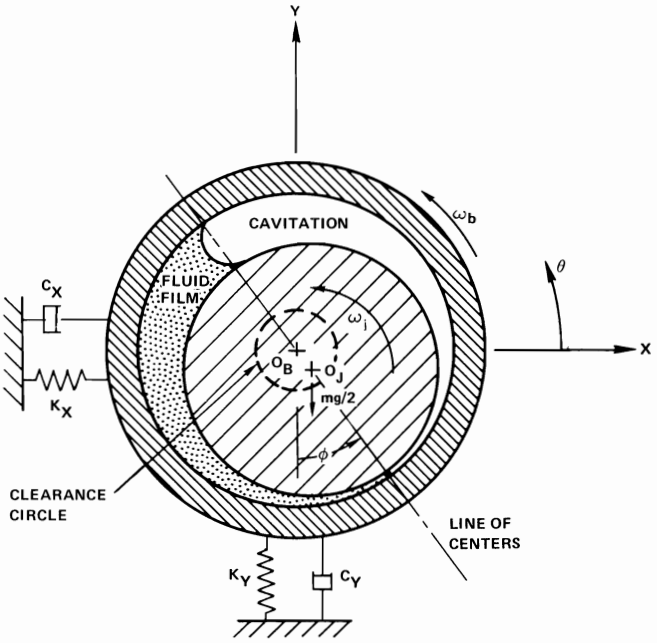

Fig. 1 Cross-section of rigid rotor system showing fluid-film and region of cavitation

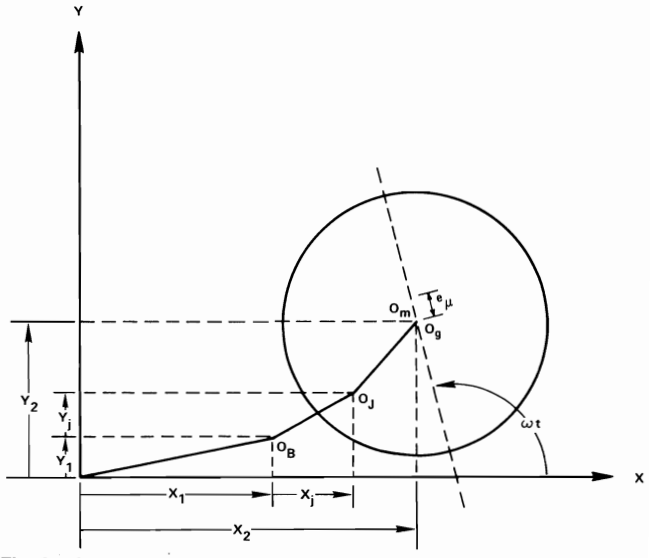

Fig. 2 Cross-section of deflected rotor at time ωt showing displacement nomenclature

section. The fluid-film will be considered to cavitate when the fluid pressure drops below the ambient pressure. In this analysis the ambient pressure level was taken to be zero. Further studies have indicated that high ambient bearing pressure levels will cause a serious reduction in the stability limits as depicted in the following stability plots, but this effect will not be included in this analysis.

The fluid film bearings are considered to be mounted in linearized, flexible, damped supports. Although the support system is considered to be linear in the stability analysis, the time-transient integration of the equations of motion may include a linear or a general nonlinear squeeze film damper system. The linearized analysis is applicable to rotors with nonlinear squeeze film damper supports which have a retainer or a preloaded retainer spring in parallel with the damper for small displacements. The damping characteristics of such a support system may be found in the literature [13, 17].

The transient response analysis of the system assumes the rotor to have an effective unbalance located at the rotor midspan and no couple unbalance moments acting along the shaft. Therefore, assuming no gyroscopic moments act on the shaft, only the cylindrical mode and not the conical mode of the shaft will be excited. Stability of this rotor system considering the conical mode has been examined by Lund [25].

Considering these restrictions, the symmetric rotor system may be described for dynamic similation by six coordinates or independent degrees of freedom. The support motion of either end of the rotor is given by the absolute coordinates X_1 and Y_1, and the bearing relative motion is denoted by (X_j, Y_j) in the fixed coordinate system. The rotor motion at the midspan is described in the fixed coordinate system by (X_2, Y_2). If the static deflection of the rotor is much less than the journal clearance ($\delta/C < 1.0$), the rotor may be considered to be rigid and hence $(X_2, Y_2) = (X_l + X_j, Y_l + Y_j)$.

The equations of motion of the system may therefore be written as four coupled second order differential equations with the fluid film bearing forces expressed as nonlinear functions of the journal relative displacements and velocities as shown in Fig. 2.

2.2 Fluid Film Bearing Characteristics. The nonlinear fluid-film forces generated by the journal bearings may be derived by considering the solution to the general Reynolds equation. Expressed in terms of a fixed cartesian coordinate system, the Reynolds equation may be written as follows:

$$\frac{\partial}{\partial z}\left[\frac{h^3}{6\mu}\frac{\partial p}{\partial z}\right] + \frac{1}{R^2}\frac{\partial}{\partial \theta}\left[\frac{h^3}{6\mu}\frac{\partial p}{\partial \theta}\right] = (\omega_b + \omega_j)\frac{\partial h}{\partial \theta} + 2\frac{\partial h}{\partial t} \quad (1)$$

The standard solution technique for bearings having $L/D < 1$ is to neglect the term $\partial P/\partial\theta$ in equation (1). This permits an approximate solution to be written for the pressure profile. Considering ambient pressure at the bearing axial boundaries, the pressure profile is given as:

$$p(\theta,z) = \frac{3\mu z(z - L)}{h^3}\left[(\omega_b + \omega_j)(x_j \sin(\theta) - y_j \cos(\theta)) - 2(\dot{x}_j \cos(\theta) + \dot{y}_j \sin(\theta))\right] \quad (2)$$

The components of force on the journal in the x-y coordinate system may be found by integrating the pressure profile over the bearing surface. This is expressed as:

$$\left.\begin{aligned} F_x &= \int_{z=0}^{L}\int_{\theta=0}^{2\pi} p(\theta,z)R\cos(\theta)d\theta dz \\ F_y &= \int_{z=0}^{L}\int_{\theta=0}^{2\pi} p(\theta,z)R\sin(\theta)d\theta dz \end{aligned}\right\} \quad (3a)$$

Integrating the axial component, the nonlinear forces generated by the journal bearing may be expressed by the following integral:

$$\begin{Bmatrix} F_x \\ F_y \end{Bmatrix} = \frac{\mu R L^3}{2}\int_0^{2\pi} \times \frac{(\omega_b + \omega_j)(x_j \sin(\theta) - y_j \cos(\theta)) - 2(\dot{x}_j \cos(\theta) + \dot{y}_j \sin(\theta))}{(c - x_j \cos(\theta) - y_j \sin(\theta))^3}\begin{Bmatrix}\cos(\theta)\\ \sin(\theta)\end{Bmatrix} d\theta \quad (3b)$$

It may be noted that the term $\omega_b + \omega_j$ can be replaced by ω, where it is to be understood that the solution is valid for bearings having both surfaces spinning. However, caution is due when defining the dimensionless velocities for transient response calculations. If the velocity terms are to be made dimensionless using the reference spin rate of the journal (i.e., ω_j), the variables should be defined such that:

$$X_j = \frac{x_j}{c};\ Y_j = \frac{y_j}{c};\ \dot{X}_j = \frac{\dot{x}_j}{c\omega_j} = \frac{dX_j}{dT};\ \dot{Y}_j = \frac{\dot{y}_j}{c\omega_j} = \frac{dY_j}{dT};\ T = \omega_j t$$

The equation for the fluid film forces may then be expressed as:

$$\begin{Bmatrix} F_x \\ F_y \end{Bmatrix} = \frac{\mu R L^3 \omega}{2c^2}\int_0^{2\pi}$$

$$X_j \sin(\theta) - Y_j \cos(\theta)$$
$$\times \frac{-2\frac{\omega_j}{\omega}(\dot{X}_j \cos(\theta) + \dot{Y}_j \sin(\theta))}{(1 - X_j \cos(\theta) - Y_j \sin(\theta))^3} \begin{Bmatrix}\cos(\theta)\\ \sin(\theta)\end{Bmatrix} d\theta \quad (4)$$

Fluid-film cavitation is accounted for in the analysis by neglecting the contribution of negative pressures when evaluating the integral given by equation (4).

The incremental fluid-film forces may be expressed by linear stiffness and damping coefficients in the small region near the steady state equilibrium position (x_0, y_0). The incremental forces are thus expressed by

$$\delta F_x = -[K_{xx} x + C_{xx} \dot{x} + K_{xy} y + C_{xy} \dot{y}] \quad (5a)$$

$$\delta F_y = -[K_{yy} y + C_{yy} \dot{y} + K_{yx} x + C_{yx} \dot{x}] \quad (5b)$$

where

$$x = x_j - x_o; \; y_j - y_o$$

with

$$F_x = F_{xo} + \delta F_x$$
$$F_y = F_{yo} + \delta F_y$$

and

$$K_{xx} = -\frac{\partial F_x}{\partial x_j}\bigg|_{\substack{x_j=x_{0j}\\ y_j=y_{0j}}}$$
$$= \frac{-\mu R L^3 \omega}{2c^3} \int_0^{2\pi} \frac{\sin(\theta)\cos(\theta) H_o + 3\cos^2(\theta) \times (X_{oi}\sin(\theta) - Y_{oi}\cos(\theta))}{H_0^4} d\theta \quad (6a)$$

$$K_{yy} = -\frac{\partial F_y}{\partial \dot{y}_j}\bigg|_{\substack{x_j=x_{0j}\\ y_j=y_{0j}}}$$
$$= \frac{-\mu R L^3 \omega}{2c^3} \int_0^{2\pi} \frac{3\sin^2(\theta)(X_{oi}\sin(\theta) - Y_{oi}\cos(\theta)) - \sin(\theta)\cos(\theta) H_0}{H_0^4} d\theta \quad (6b)$$

$$C_{xx} = \frac{-\partial F_x}{\partial \dot{x}}\bigg|_{\substack{x_j=x_{0j}\\ y_j=y_{0j}}} = \frac{\mu R L^3}{2c^3} \int_0^{2\pi} \frac{2\cos^2(\theta)}{H_0^3} d\theta \quad (6c)$$

$$C_{yy} = \frac{-\partial F_y}{\partial \dot{y}}\bigg|_{\substack{x_j=x_{0j}\\ y_j=y_{0j}}} = \frac{\mu R L^3}{2c^3} \int_0^{2\pi} \frac{2\sin^2(\theta)}{H_0^3} d\theta \quad (6d)$$

$$K_{xy} = \frac{-\partial F_x}{\partial y}\bigg|_{\substack{x_j=x_{0j}\\ y_j=y_{0j}}}$$
$$= \frac{\mu R L^3 \omega}{2c^3} \int_0^{2\pi} \frac{3\sin(\theta)\cos(\theta)(X_{oi}\sin(\theta) - Y_{oi}\cos(\theta)) - H_0\cos^2(\theta)}{H_0^4} d\theta \quad (6e)$$

$$K_{yx} = \frac{-\partial F_y}{\partial x}\bigg|_{\substack{x_j=x_{0j}\\ y_j=y_{0j}}}$$
$$= \frac{-\mu R L^3 \omega}{2c^3} \int_0^{2\pi} \frac{3\sin(\theta)\cos(\theta)(X_{oj}\sin(\theta) - Y_{oj}\cos(\theta)) + H_0\sin^2(\theta)}{H_0^4} \quad (6f)$$

$$C_{xy} = \frac{-\partial F_x}{\partial \dot{y}}\bigg|_{\substack{x_j=x_{0j}\\ y_j=y_{0j}}} = \frac{\mu R L^3}{2c^3} \int_0^{2\pi} \frac{2\sin(\theta)\cos(\theta)}{H_0^3} d\theta \quad (6g)$$

$$C_{yx} = \frac{-\partial F_y}{\partial \dot{x}}\bigg|_{\substack{x_j=x_{0j}\\ y_j=x_{0j}}} = \frac{\mu R L^3}{2c^3} \int_0^{2\pi} \frac{2\sin(\theta)\cos(\theta)}{H_0^3} d\theta \quad (6h)$$

These integrals are to be calculated over the area of positive pressure which is present under steady state conditions.

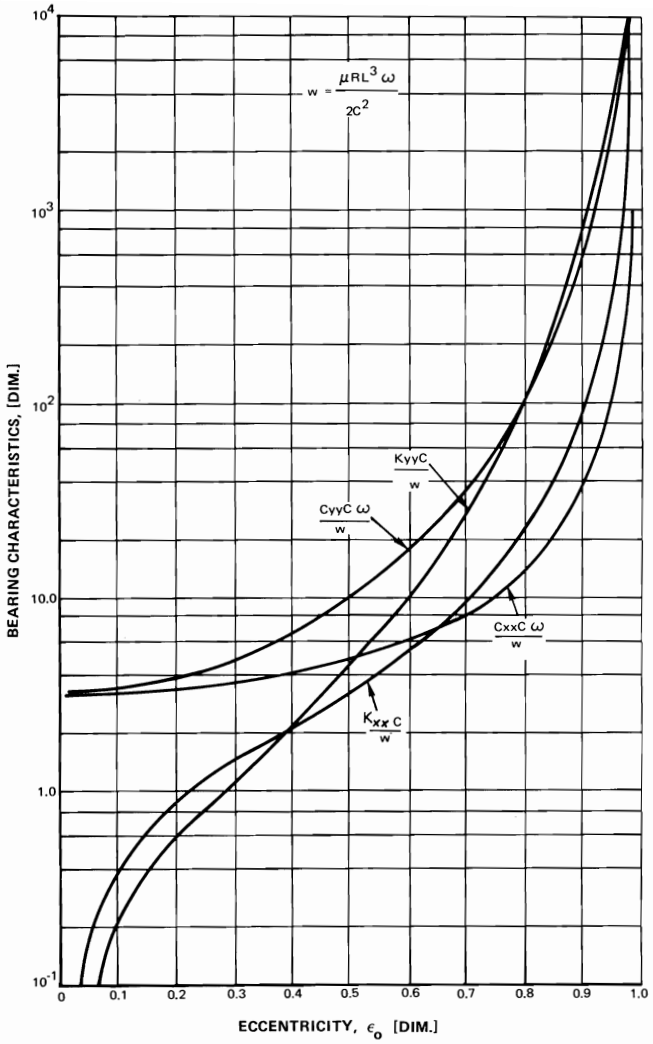

Fig. 3 Dimensionless direct stiffness and damping coefficients for the short journal bearing

The steady state equilibrium position ϵ_0, may be found for any load by an iterative routine using the Ocvirk number [19] which is expressed as:

$$S_s = \frac{\mu N}{P}\left(\frac{R}{c}\right)^2\left(\frac{L}{D}\right)^2 = \frac{(1-\epsilon^2)^2}{\pi\epsilon[\pi^2(1-\epsilon^2) + 16\epsilon^2]^{1/2}} \quad (7)$$

where

$$P = \frac{\text{bearing load}}{L \times D}$$

N = bearing effective speed (rev./s)

Hence, for a given bearing geometry, load, and speed the equilibrium position is expressed as:

$$X_{oj} = \epsilon_0 \sin(\phi_0)$$
$$Y_{oj} = -\epsilon_0 \cos(\phi_0) \quad (8)$$

where:

$$\phi_0 = \text{attitude angle} = \tan^{-1}\left[\frac{\pi}{4}\frac{\sqrt{1-\epsilon_0^2}}{\epsilon_0}\right] \quad (9)$$

and ϵ_0 is found by using equation (7).

The bearing characteristics may therefore be expressed as dimensionless values as a function of eccentricity and the resulting values are shown in Figs. 3 and 4. These bearing characteristics have been used in generating the stability boundaries in the following section of this paper.

Fig. 3 represents the direct or principal stiffness and damping

values for a short journal bearing with a cavitated film. The bearing characteristics obtained can be shown to be in close agreement with the characteristics reported by various investigators such as Holmes [27], Lund [25], and Badgley [11]. It is of interest to note that as the eccentricity ϵ_0 reduces, the principal stiffness terms K_{xx} and K_{yy} rapidly reduce, approaching 0 in the limit as ϵ_0 approaches O while the principal damping values C_{xx} and C_{yy} approach an asymptotic limit. Poritsky [26] was the first to recognize that the journal bearing must have a radial restoring spring rate in order to have a finite stability threshold. The conditions that the principal stiffness terms K_{xx} and K_{yy} must be positive for a finite stability threshold to exist is also given in reference [9]. If the journal is operating at zero eccentricity, or if the bearing film is not allowed to cavitate, then the principal stiffness terms vanish, and the journal is inherently unstable and the system will exhibit half frequency whirl. Threefore if a flexible damper support is incorporated with a vertical journal bearing or an uncavitated bearing, the system will still be unstable, however the size of the resulting limit cycle orbits will be greatly reduced.

Fig. 4 represents the cross-coupled stiffness and damping coefficients. Examination of the general stability criteria of reference [9] indicate that the cross-coupling terms K_{xy} and K_{yx} are the major sources of instability and that the cross coupled damping terms play only a minor roll in determining the stability threshold. In order to generate instability, the cross-coupling term K_{yx} must be negative and the greatest degree of instability occurs when K_{xy} is of equal and opposite sign to K_{yx}. When K_{xy} becomes negative also, the system stability rapidly improves as shown in Fig. 5.

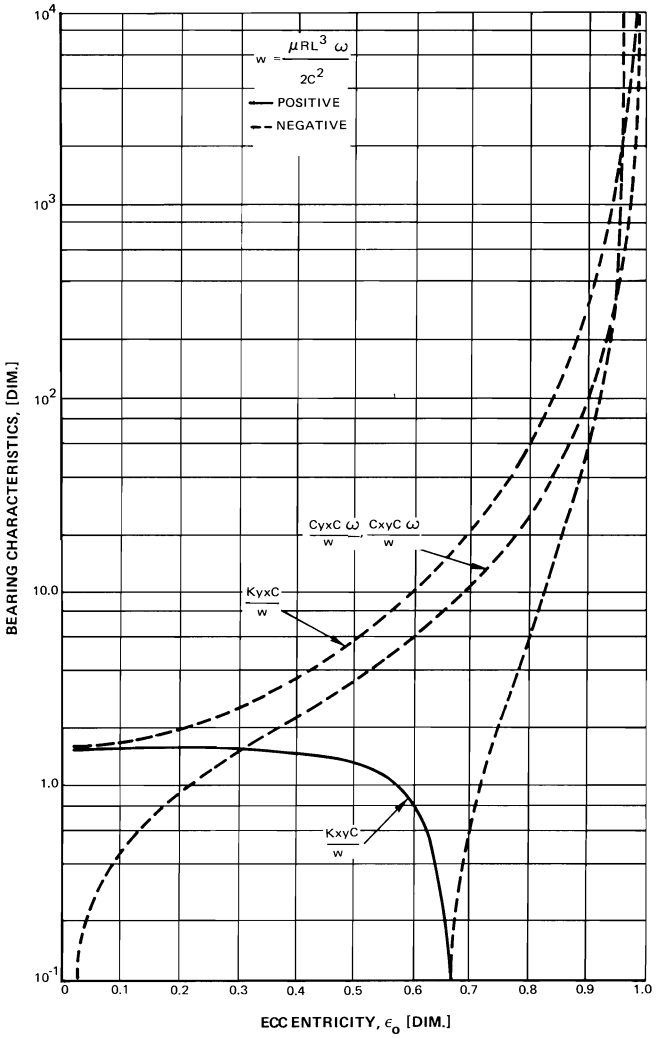

Fig. 4 Cross-coupled stiffness and damping coefficients for the short journal bearing

2.3 Equations of Motion. The equations of motion for the symmetric rotor system as shown in Fig. 1 may be expressed as follows with the rotor characterized by a shaft stiffness, K_s, and absolute damping, C_s.

Rotor:

$$m_2\ddot{x}_2 + K_s(x_2 - x_j - x_1) + C_s\dot{x}_2 = m_2 e_{\mu_2}\omega_j^2 \cos(\omega_j t) + f_x(t) \quad (10a)$$

$$m_2\ddot{y}_2 + K_s(y_2 - y_j - y_1) + C_s\dot{y}_2 = m_2 e_{\mu_2}\omega_j^2 \sin(\omega_j t) - m_2 g + f_y(t) \quad (10b)$$

Journal:

$$m_j(\ddot{x}_j + \ddot{x}_1) - F_x(x, y, \dot{x}, \dot{y})_j - \frac{K_s}{2}(x_2 - x_j) = 0 \quad (11a)$$

$$m_j(\ddot{y}_j + \ddot{y}_1) - F_y(x, y, \dot{x}, \dot{y})_j - \frac{K_s}{2}(y_2 - y_j - y_1) = m_j g \quad (11b)$$

Support:

$$m_1\ddot{x}_1 + F_x(x, y, \dot{x}, \dot{y})_j + K_{1xx}x_1 + K_{1xy}y_1 + C_{1xx}\dot{x}_1 + C_{1xy}\dot{y}_1 = F_{p_x} \quad (12a)$$

$$m_1\ddot{y}_1 + F_y(x, y, \dot{x}, \dot{y})_j + K_{1yy}y_1 + K_{1yx}x_1 + C_{1yy}\dot{y}_1 + C_{1yx}\dot{x}_1 = -m_1 g + F_{p_y} \quad (12b)$$

where

C_s = absolute damping on rotor midspan
$\vec{f}(t)$ = any time dependent or steady loading acting on the rotor (including effects of aerodynamic loading or internal friction)
$\vec{F}_p$ = preload force on the bearing support system
$\vec{F}(x, y, \dot{x}, \dot{y})_j$ = fluid-film forces expressed by equation (3).

If the rotor shaft stiffness may be considered to the rigid ($m_2 g/K_s \ll c$) then the equation may be reduced still further to the following system of equations.

$$m(\ddot{x}_1 + \ddot{y}_j) - F_x(x, y, \dot{x}, \dot{y})_j = m\epsilon_\mu \omega^2{}_j \cos(\omega_j t) + 1/2 f_x(t) - 1/2 C_s(\dot{x}_1 + \dot{x}_j) \quad (13a)$$

$$m(\ddot{y}_1 + \ddot{y}_j) - F_y(x, y, \dot{x}, \dot{y})_j = m\epsilon_\mu \omega^2{}_j \sin(\omega_j t) + 1/2 f_y(t) - mg - 1/2 C_s(\dot{y}_1 + \dot{y}_j) \quad (13b)$$

$$m_1\ddot{x}_1 + F_x(x, y, \dot{x}, \dot{y})_j + K_{1xx}x_1 + K_{1xy}y_1 + C_{1xx}\dot{x}_1 + C_{1xy}\dot{y}_1 = F_{p_x} \quad (14a)$$

$$m_1\ddot{y}_1 + F_y(x, y, \dot{x}, y)_j + K_{1yy}y_1 + K_{1yx}x_1 + C_{1yy}\dot{y}_1 + C_{1yx}\dot{x}_1 = F_{py} - m_1 g \quad (14b)$$

These are the equations required for time transient response calculations. For stability consideration, the homogeneous equation written about the steady state equilibrium position may be expressed in dimensionless form considering the bearing characteristics as given by equation (5). The cross-coupling terms for the flexible support are neglected to reduce the number of variables in the analysis. The resulting equations are expressed as follows:

$$(1 + \delta m)X_1'' + \overline{C}_x X_1' + \overline{K}_x X_1 + X_2'' = 0 \quad (15a)$$

$$(1 + \delta m)Y_1'' + C_y Y_1' + K_y Y_1 + Y_2'' = 0 \quad (15b)$$

$$X_1'' + X_j'' + K_{xx}x_j + C_{xx}X_j' + K_{xy}Y_j + C_{xy}Y_j' = 0 \quad (15c)$$

$$Y_1'' + Y_j'' + \overline{K}_{yy}Y_j + \overline{C}_{yy}Y_j' + \overline{K}_{yx}X_j + \overline{C}_{yx}X_j' = 0 \quad (15d)$$

The support characteristics are assumed to be symmetric to further reduce the number of dimensionless parameters in the study. Thus the extent of the stable region will be the lowest obtainable since bearing support asymmetry will in general increase the stable operating speed range. The following dimensionless support characteristic variables are defined.

$$\overline{K}_B = K_B/m\omega_g^2;\ K_B = K_{1xx} = K_{1yy}$$
$$\overline{C}_B = C_B/m\omega_g;\ C_B = C_{1xx} = C_{1yy} \tag{16}$$

where

$$\omega_g = \sqrt{\frac{W}{mc}}$$

The stability of the rotor system may now be calculated in terms of the dimensionless parameters given in the preceding discussion. From the above dimensionless parameters, it may be shown that the stability threshold speed may be expressed as

$$\omega\Big|_{\substack{\text{Threshold}\\ \text{Speed}}} = f\left(\sqrt{\frac{W}{mc}},\ \delta m,\ \epsilon,\ \overline{K}_B,\ \overline{C}_B\right) \tag{17}$$

These parameters will be used to plot the results of the stability analysis presented in the following discussion.

3 Stability and Transient Motion on Rigid Supports

3.1 Journal Bearing Stability. The stability analysis of the nonlinear rotor-bearing system is obtained by employing the linearized equations of motion of the balanced rotor about the steady state equilibrium position.

The case of the journal bearing on rigid supports reduces the equations of motion to a system of two degrees of freedom. In Fig. 5, the stability threshold of the isolated two degrees of freedom journal bearing is presented in terms of the stability parameter ω_s vs the bearing equilibrium eccentricity ratio ϵ. The results of this elementary system is compared with the results generated by Badgley-Booker [20] who also assumed the short bearing approximation. The stability profile generated by the evaluation of the bearing characteristics in fixed cartesian coordinates is in excellent agreement with the results shown by Badgley and Booker. Also shown for comparison is the stability boundary generated by Reddi-Trumpler [21] for the 180-deg bearing with end leakage. This analysis indicates a decreasing threshold speed for decreasing eccentricities.

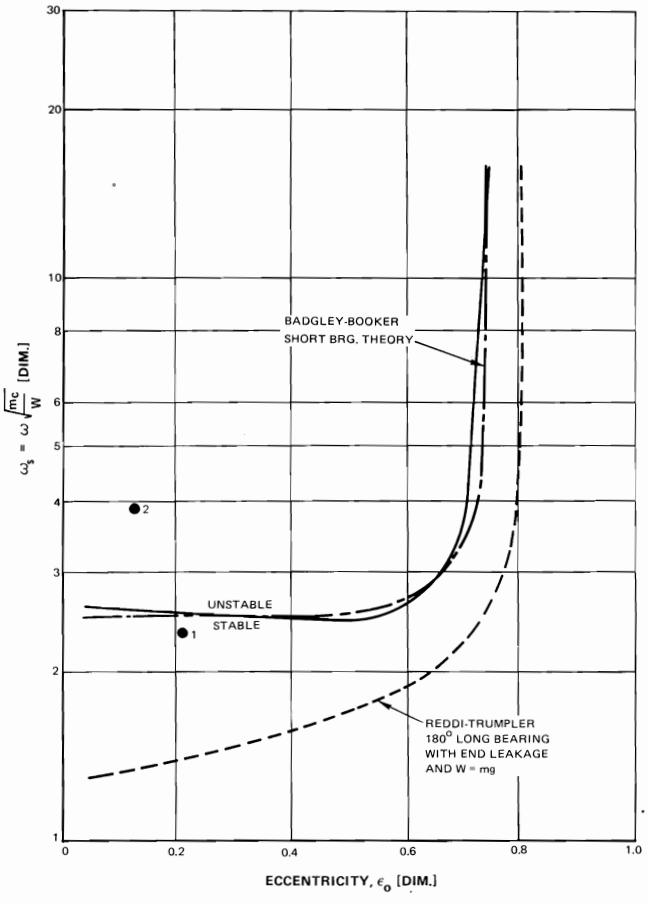

Fig. 5 Stability map for the short journal bearing with rigid supports

The stability of the finite width bearing for various aspect ratios of L/D was treated by Lund [25]. Comparison of these profiles indicates that the short bearing theory predicts accurate stability boundaries for aspect ratios of ($L/D \leq 0.5$).

Lund also shows that for large aspect ratios ($L/D = 2.0$) the characteristic stability curve is similar to the approximate stability boundary first presented by Reddi-Trumpler which shows that the stability decreases with decreasing eccentricity. However the asymplotic value that Lund obtained for $L/D = 2.0$ approaches 2.17 rather than the lower value of 1.3 as shown Reddi.

The stability boundary of the present analysis is found to decrease slightly with increasing eccentricity. The minimum threshold of stability is obtained at an eccentricity of $\epsilon_0 = 0.5$ and the value of ω_s is approximately 2.5. As the steady-state eccentricity increases beyond 0.5, the stability rapidly increases, until the system is completely stable beyond $\epsilon_0 = 0.7$, which also agrees with the results stated by Hori [10].

Example 1

Determination of the journal stability $-N = 6500$ rpm

Given $W = 50$ lb (22.68 kg),
$R = 1.00$ in. (2.54 in.)
$L = 1.00$ in. (2.54 cm)
$\mu = 1.0 \times 10^{-5}$ Reyns
$C = 0.005$ in.

From the above data the bearing Sommerfeld number may be calculated and hence the steady state eccentricity ratio can be determined.

$$S = \frac{\mu N_s}{W} LD \left(\frac{R}{C}\right)^2 = \frac{1 \times 10^{-5} \times 108.33}{50} \times 1 \times 2 \times \left(\frac{1}{.005}\right)^2$$

$$S = 1.733 = \left(\frac{D}{L}\right)^2 \frac{(1-\epsilon^2)^2}{\pi\epsilon[\pi^2(1-\epsilon^2) + 16\epsilon^2]^{1/2}}$$

By the Newton-Raphson iteration the equilibrium eccentricity is found to be $\epsilon_0 = 0.211$. From the stability plot (at Point 1) the stability threshold is approximately $\omega_s = 2.5$. The rotor operating speed parameter $\omega_s{}^*$ is given by

$$\omega_s{}^* = \omega\sqrt{\frac{MC}{g}} = 680.68\sqrt{\frac{0.005}{386}} = 2.45$$

Since the operating speed is below the stability threshold, the system should be stable about the steady-state equilibrium position of $\epsilon_0 = 0.211$.

Fig. 6*(a)* represents the transient path of the journal corresponding to the conditions in Example 1.

3.2 Journal Bearing Transient Motion. Although the stability analysis of the linearized system is needed in order to establish the stable operating boundaries of the system, it does not answer the important question as to the magnitude of the unstable orbit. For example, two rotors may have a similar threshold of stability, yet one may have considerably better operating characteristics in that it has smaller limit cycle orbits above the stability threshold. The question of the actual nonlinear rotor motion above the stability threshold and also the influence of rotor imbalance on the motion of the system can only be answered by a time-transient method of analysis in which the nonlinear equations of motion are inte-

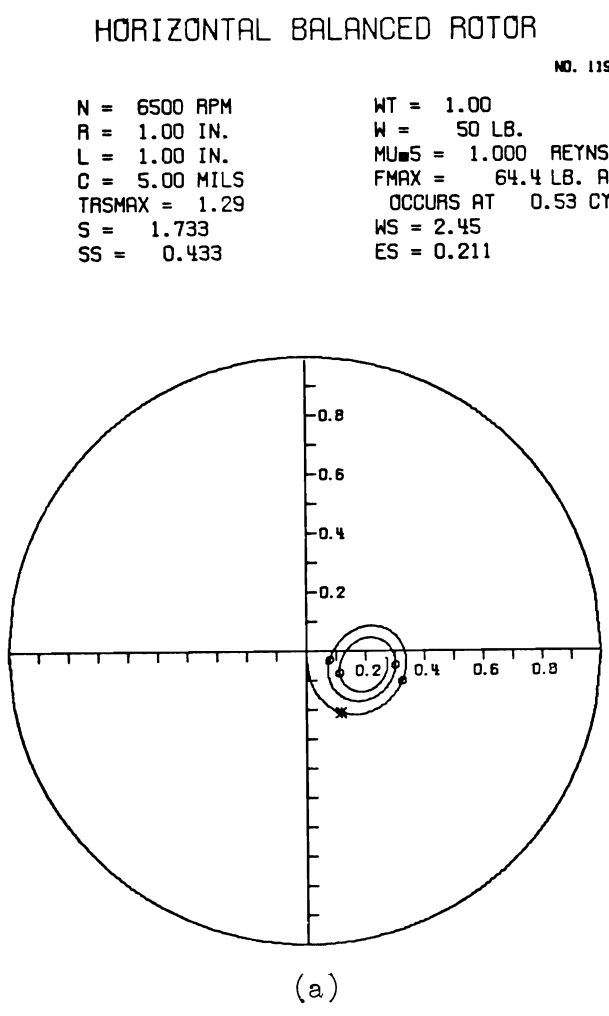

Fig. 6*(a)* Journal orbit of a balanced horizontal rotor on rigid supports (*N* = 6500 rpm, *W* = 50 lb. (22.68 kg), *C* = 0.005 mils (0.0127 cm), *L/D* = ½)

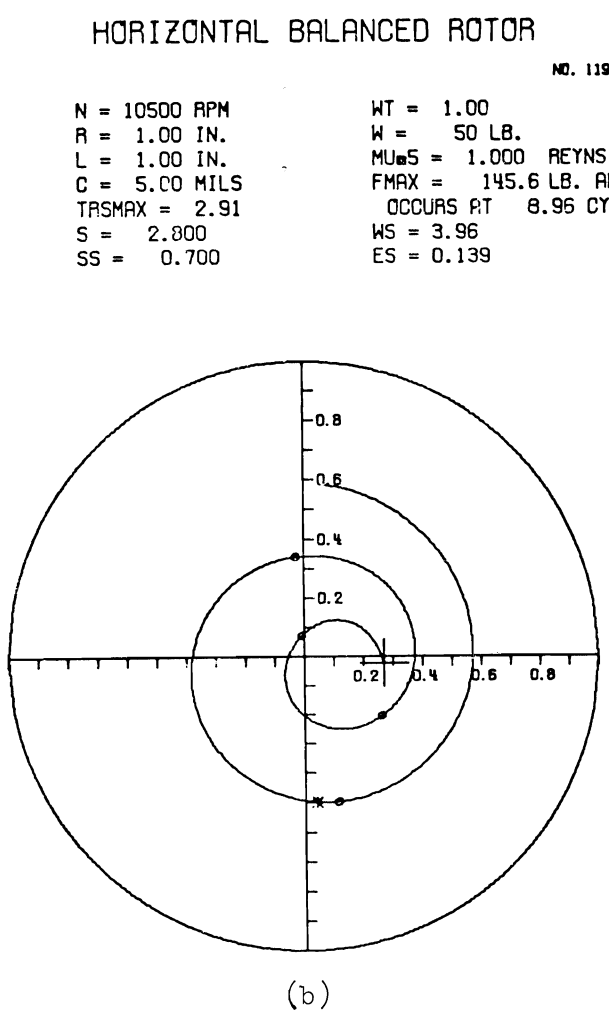

Fig. 6*(b)* Journal orbit of a balanced rotor for cycles 6–10 (*N* = 10,500 rpm)

grated forward in time. It should be noted that the use of a time-transient program without a corresponding linearized stability plot has proven to be costly and time consuming as it is not apparent from the observation of the transient orbits alone as to what support or bearing parameters will promote optimum stability. The analysis of the time transient motion of journal bearings is given in detail in references [11 and 22].

The typical characteristics of a rotor operating below the stability threshold speed is shown in Fig. 6*(a)*. The transient path of the journal is plotted in the reference clearance circle. The rotor is operating at 6500 rpm and at time $t = 0$, the rotor is dropped from the center ($X = Y = 0$). The resulting path of the journal is indicated to be stable and spiraling into the equilibrium eccentricity ($\epsilon_0 = ES = 0.211$). The small circles on the orbit indicate one spin revolution of the rotor. The asterisk on the orbit is the point of maximum load transmitted and for this case it is indicated to be 64.4 lb. (286.45 N.)

If the system properties are used to calculate the position on the stability map of Fig. 5, the point labeled 1 is obtained as shown in Example 1. The system is thus seen to be operating just below the threshold speed. An increase of rotor speed to 10,500 rpm gives the position on the map labeled 2 which is seen to be unstable. This is shown clearly in Figs. 6*(b)* and 6*(c)* where the journal is spiraling outward at a whirl rate very close to one-half operating speed.

The response of a fluid-film bearing is typically plotted as the motion of the geometric center of the journal in the clearance circle. This is equivalent to the orbit trace that would be observed on an oscilloscope showing the output of displacement probes mounted on the bearing support and monitoring the journal motion. The physical interpretation of an instability is demonstrated in Fig. 6*(b)* where the rotor speed is 10,500 rpm (Point 2 on Fig. 5). The rotor is spiraling outward at a very high growth rate. In five revolutions of the shaft the response has doubled. Thus the average growth rate, a, for this system is calculated to be:

$$R = R_0 e^{at};\ l = 0.005714 \text{ s/rev}$$

therefore,

$$\frac{R}{R_0} = 2.0 = e^{a(.02857)}$$

and hence

$$a = 24.26$$

The continuation of the motion for another five cycles is shown in Fig. 6*c*. The growth rate is greatly reduced ($a = 8.53$) and a limit cycle is formed which is as expected for the nonlinear system. The stability analysis which uses linearized equations cannot predict the limit cycle condition as was shown in the transient orbit.

The analysis of imbalance response in a nonlinear system may be obtained by transient response techniques. The mass of the rotor is considered to be displaced from the geometric center by an amount $E_\mu = EMU = e_{\mu/c}$ where c is the radial clearance of the bearing. Consider initially a rigid support system and an imbalance given as $EMU = 0.20$. For a rotor speed of 6500 rpm the orbit is shown in Fig. 7*(a)* for the case of a suddenly applied imbalance and release of the journal from $x = y = 0$ at the time $t = 0$. The re-

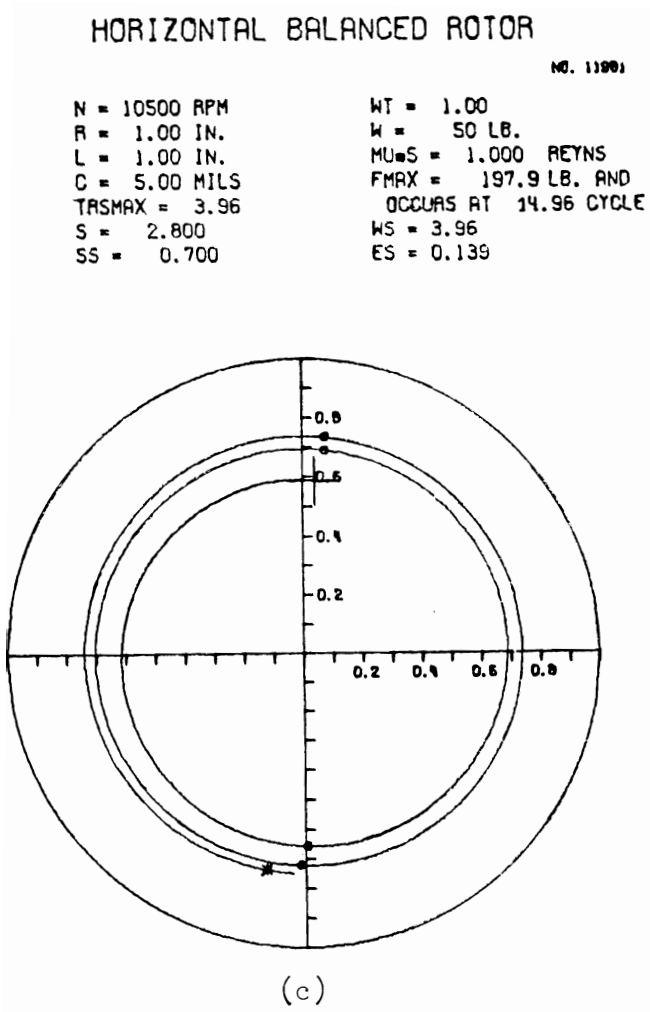

Fig. 6*(c)* Journal orbit of a balanced rotor for cycles 11–15 showing motion near limit cycle (*N* = 10,500 rpm)

sponse has both synchronous and non-synchronous components but at the end of only five cycles of motion the system is reducing to predominantly a synchronous response. An increase of rotor speed to 10,500 rpm (above the threshold speed) produces the unstable orbit shown in Fig. 7*(b)*.

4 Stability and Transient Motion on Flexible Supports

4.1 STABILITY ANALYSIS. The equations of motion as presented in equation (15) may be analyzed for stability by examination of the system characteristic equation. Assuming solutions of the form $X = \bar{X}e^{\lambda t}$, the following characteristic determinant may be written.

$$\begin{vmatrix} (1+\delta m)\lambda^2 + \bar{C}_x\lambda + \bar{K}_x & 0 & \lambda^2 & 0 \\ 0 & (1+\delta m)\lambda^2 + \bar{C}_y\lambda + \bar{K}_y & 0 & \lambda^2 \\ \lambda^2 & 0 & \lambda^2 + \bar{C}_{xx}\lambda + \bar{K}_{xx} & \bar{C}_{xy}\lambda + \bar{K}_{xy} \\ 0 & \lambda^2 & \bar{C}_{yx}\lambda + \bar{K}_{yx} & \lambda^2 + \bar{C}_{yy}\lambda + \bar{K}_{yy} \end{vmatrix} = 0 \quad (18)$$

The resulting eighth-order polynomial in λ may be expressed as [16]

$$A_0\lambda^8 + A_1\lambda^7 + A_2\lambda^6 + \ldots + A_7\lambda + A_8 \quad (19)$$

where

$$A_i = \alpha_i + \beta_i;\ i = 0, 1, 2, \ldots, 7, 8 \quad (20)$$

and

$$\alpha_i = (1 + \delta m)a_{i+2} + \bar{C}_x a_{i+1} + \bar{K}_x a_{i+2};\ i = 0, 1, 2, \ldots 7, 8 \quad (21)$$

with

$$a_0 = a_1 = 0$$

$$a_2 = \delta m$$

$$a_3 = \bar{C}_y + \bar{C}_{yy} + \delta m(\bar{C}_{xx} + \bar{C}_{yy})$$

$$a_4 = \bar{K}_y + \bar{K}_{yy} + \bar{C}_{xx}\bar{C}_{yy} - \bar{C}_{xy}\bar{C}_{yx} + \delta m(\bar{K}_{xx} + \bar{K}_{yy} + \bar{C}_{xx}\bar{C}_{yy} - \bar{C}_{xy}\bar{C}_{yx}) + \bar{C}_y(\bar{C}_{xx} + \bar{C}_{yy})$$

$$a_5 = (1 + \delta m)[\bar{C}_{yy}\bar{K}_{xx} + \bar{C}_{xx}\bar{K}_{yy} - \bar{C}_{yx}\bar{K}_{xy} - \bar{C}_{xy}\bar{K}_{yx}] + \bar{C}_y[\bar{K}_{xx} + \bar{K}_{yy} + \bar{C}_{xx}\bar{C}_{yy} - \bar{C}_{xy}\bar{C}_{yx}] + \bar{K}_y[\bar{C}_{xx} + \bar{C}_{yy}]$$

$$a_6 = (1 + \delta m)[\bar{K}_{xx}\bar{K}_{yy} - \bar{K}_{xy}\bar{K}_{yx}] + \bar{C}_y[\bar{C}_{yy}\bar{K}_{xx} + \bar{C}_{xx}\bar{K}_{yy} - \bar{C}_{yx}\bar{K}_{xy} - \bar{C}_{xy}\bar{K}_{yx}]$$

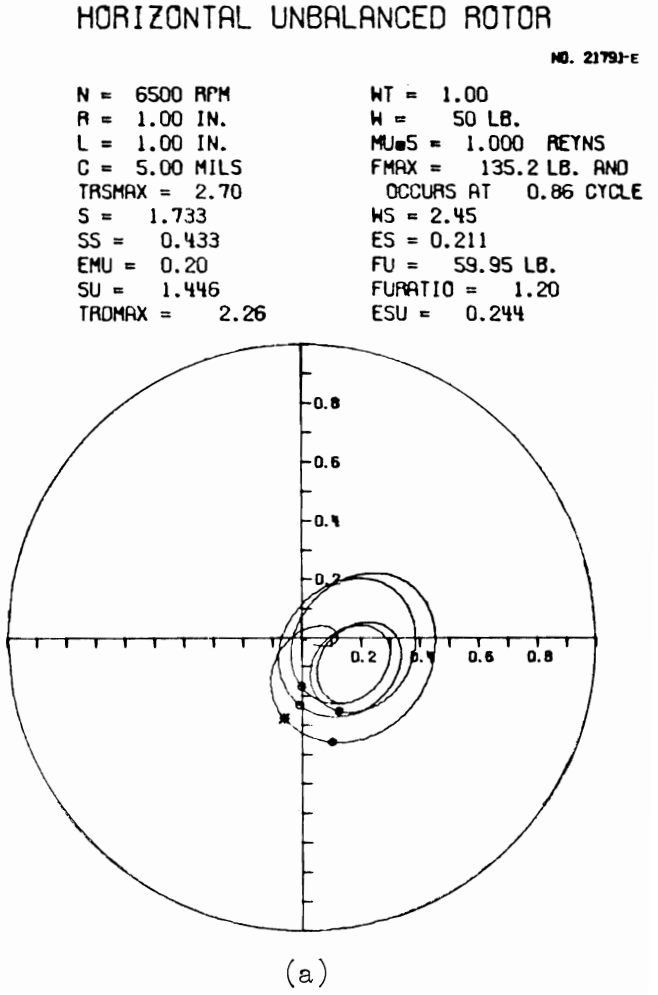

Fig. 7*(a)* Journal orbit of an unbalanced rotor on rigid supports for five cycles (*N* = 6500 rpm, *W* = 50 lb. (22.68 kg), *C* = 0.005 mils (0.0127 cm.), *L/D* = ½, *Eμ* = 0.2)

$$+ \bar{K}_y[\bar{K}_{xx} + \bar{K}_{yy} + \bar{C}_{xx}\bar{C}_{yy} - \bar{C}_{xy}\bar{C}_{yx}]$$

$$a_7 = \bar{C}_y[\bar{K}_{xx}\bar{K}_{yy} - \bar{K}_{xy}\bar{K}_{yx}] + \bar{K}_y[\bar{C}_{yy}\bar{K}_{xx} + \bar{C}_{xx}\bar{K}_{yy} - \bar{C}_{yx}\bar{K}_{xy} - \bar{C}_{xy}\bar{K}_{yx}]$$

$$a_8 = \bar{K}_y[\bar{K}_{xx}\bar{K}_{yy} - \bar{K}_{xy}\bar{K}_{yx}]$$

Also,

$$\beta_0 = -\delta m$$

$$\beta_1 = -\bar{C}_y - \bar{C}_{yy}(1 + \delta m)$$

$$\beta_2 = -\bar{K}_y - \bar{C}_y\bar{C}_{yy} - (1 + \delta m)\bar{K}_{yy}$$

$$\beta_3 = -\bar{K}_y\bar{C}_{yy} - \bar{C}_y\bar{K}_{yy}$$

$$\beta_4 = -\bar{K}_y\bar{K}_{yy}$$

$$\beta_i = 0,\ i = 5, 6, 7, 8$$

The characteristic equation given by equation (19) may be examined by the Routh criteria [16] to determine the onset of instability. The equations were programmed on a digital computer and an extensive study of the lowest stability threshold speed was determined for various values of dimensionless support parameters. The results of this investigation are plotted as a dimensionless stability parameter, $\omega_s = \omega\sqrt{mc/W}$, versus the dimensionless steady state equilibrium position of the journal which is denoted as ϵ_0. For the horizontal rotor system under 1-g loading the stability parameter reduces to $\omega_s = \omega\sqrt{c/g}$. This parameter has been widely used to express the stability of short journal bearings [11, 14, 20, 21]. The equilibrium position of the journal may be expressed in terms of the Ocvirk number, S_s. In addition, it is easily shown that

$$\omega\sqrt{\frac{mc}{W}} = \bar{W}\,S_s \tag{22}$$

where

$$\bar{W} = \frac{2\pi W}{\mu LD}\left(\frac{2c}{L}\right)^2\sqrt{\frac{mc}{W}} \tag{23}$$

This parameter is defined as the load number of the bearing and may be used on the stability map to determine the operating eccentricity for a given rotor bearing configuration.

The stability map shown as Fig. 8 was plotted for a specified value of support stiffness, $\bar{K}_B$, and mass ratio, $\delta m = m_1/m$. Stability boundaries for numerous values of support damping are shown on the figure to illustrate the effect of damping on the threshold speed. For example, Fig. 8 indicates that (for $\bar{K}_B = 0.1$, $\delta m = 0.1$) the threshold speed may be raised significantly above the rigid support threshold speed (shown as dash-dot line) for a damping value of $\bar{C}_B \sim 0.5$. In addition, it is easily observed that a lightly damped support system ($C_B \sim 0.001$) reduces the onset of instability for bearings having $\epsilon_0 < 0.7$. This effect will be examined in greater detail later in the discussion.

The load lines indicated by dashed lines trace the journal eccentricity of a rotor as the running speed is increased or decreased. For heavily loaded journals ($\bar{W} > 100$) it is evident that the stability is greatly increased beyond the corresponding onset speed for a lightly loaded journal ($\bar{W} < 50$). The stability map also indicates an optimum damping value for maximum increase of the stable

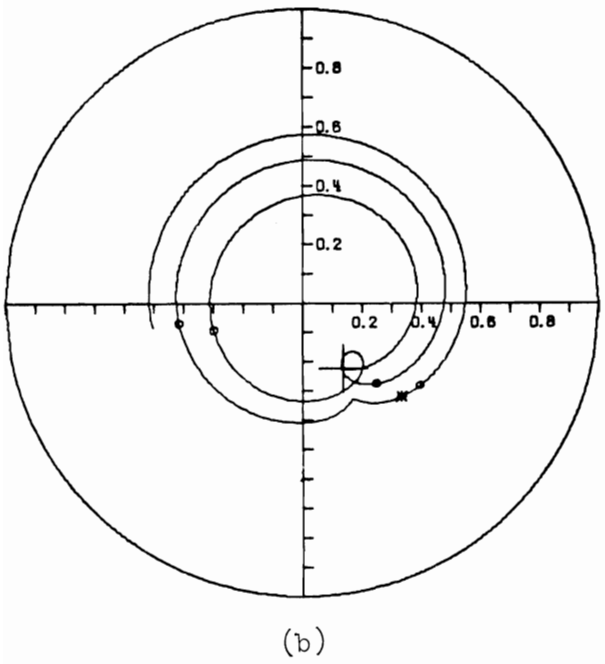

(b)

Fig. 7(b) Journal orbit of an unbalanced rotor above the stability threshold speed (N = 10,500 rpm, ω_s = 3.96)

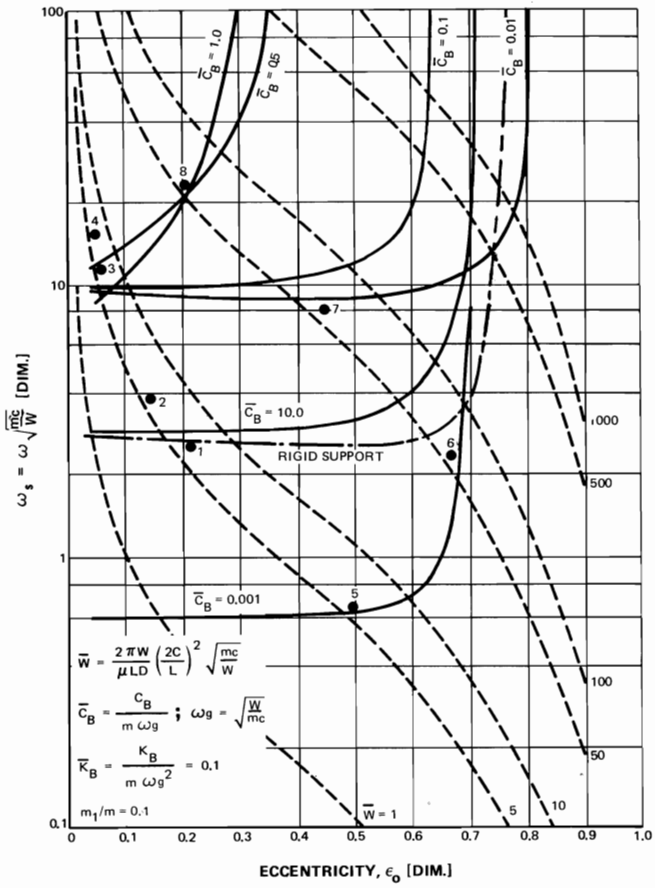

Fig. 8 Stability map for the damped, flexible support rotor on short journal bearings ($\bar{K}_B = 0.1$, $m_1/m = .1$)

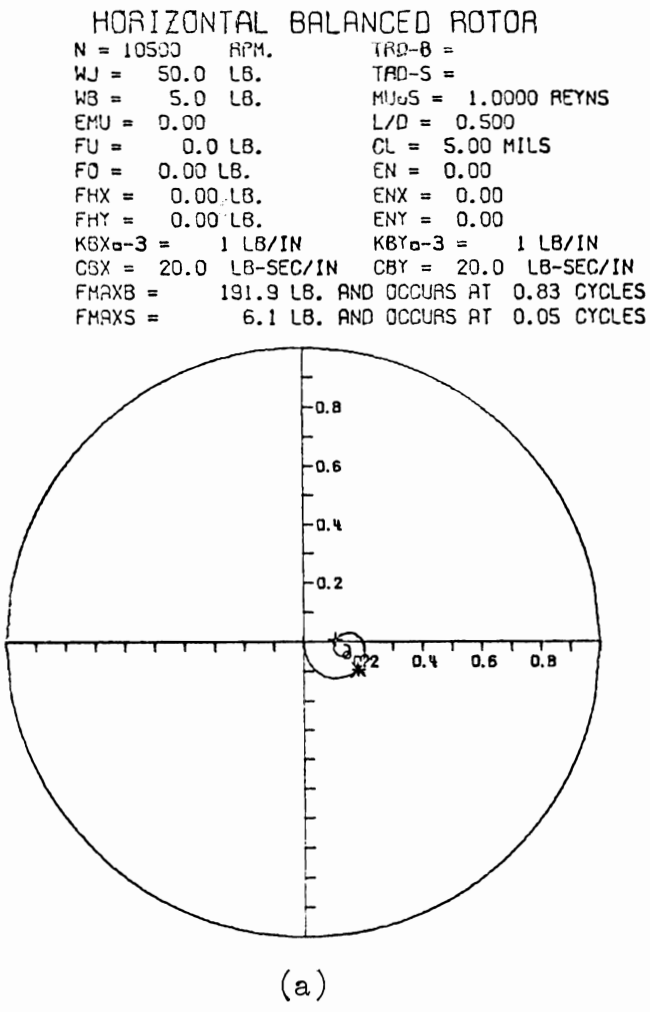

Fig. 9*(a)* Rotor relative motion showing stabilized response (N = 10,500 rpm, ω_s = 3.96)

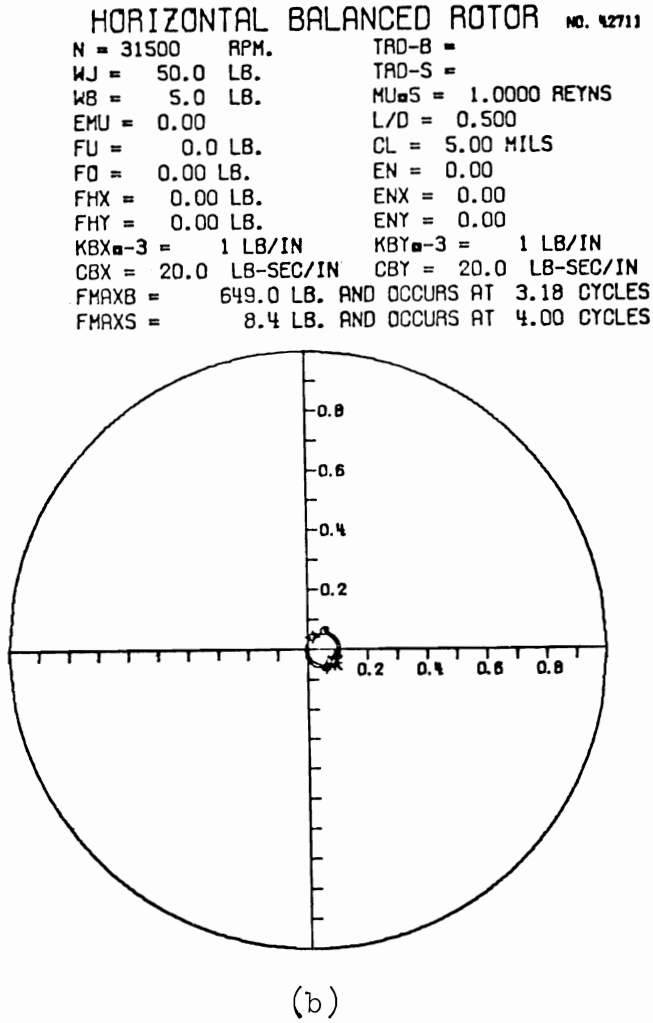

Fig. 9*(b)* Rotor relative motion at the threshold of stability (N = 31,500 rpm, ω_s = 11.9)

operating speed range. An overdamped support system (C_B > 10.0), reduces the threshold speed to the rigid support onset speed.

Consider the following rotor system which will be used to illustrate the effects of support properties on stability and transient response.

Example 2:

rotor weight—50 lb (22.68 kg)
journal weight (each)—25 lb (11.34 kg)
journal radius—1 in. (2.54 cm)
journal clearance—.005 in. (.0127 cm)
support weight (each)—5.0 lb (2.268 kg)
support stiffness—1000.0 lb/in. (1751.26 N/cm)
support damping—20 lb-s/in. (35.03 N-s./cm)
viscosity—1.0×10^{-5} Reyns

This rotor system produces the following dimensionless values:

$$\delta m = 5.0/[(50 + 2(25))/2] = 0.1$$

$$K_B = \frac{1000.0}{\frac{50}{386}\left(\frac{50\,(386)}{50\,(.005)}\right)} = 0.1$$

$$C_B = \frac{20}{\frac{50}{386}\sqrt{\frac{50\,(386)}{50\,(.005)}}} = 0.556$$

$$W = \frac{2\pi\,(50)}{1 \times 10^{-5}(1)(2)}\left(\frac{.010}{1}\right)^2\sqrt{\frac{50\,(.005)}{386\,(50)}} = 5.65$$

If the rotor speed is 10,500 rpm the previous discussion of rigid support bearings indicated that the rotor would be unstable. The stability parameter is calculated to be:

$$\omega_s = 10500\left(\frac{2\pi}{60}\right)/\sqrt{\frac{50\,(386)}{50\,(.005)}} = 3.96$$

The equilibrium eccentricity is calculated to be 0.139 and the point labeled 2 on Fig. 8 indicates the system with the damped support giving $\bar{C}_B$ = 0.556 should be very stable. The transient response of the balanced rotor is shown in Fig. 9*(a)*. The rotor is indicated to be very stable as shown by the rapid decay of the transient to the steady state eccentricity. An increase of rotor speed to 31,500 rpm produces the Point 3 on Fig. 8 and is very near the threshold speed. This is clearly indicated by the transient response shown as Fig. 9*(b)* where the journal continues to orbit at approximately half-frequency indicating near zero damping at this speed. An increase of speed to 45,00 rpm places the journal above the threshold as shown by Point 4 of Fig. 8. The response for this condition is given in Fig. 9*(c)* and the motion is growing exponentially and would eventually grow into a large limit cycle response. The support system has increased the stability threshold speed by a factor of 4.75 beyond the rigid support threshold speed.

The effect of decreasing the support stiffness, $\bar{K}_B$ = 0.01 is shown in Fig. 10*(a)* and it is indicated that for values of damping $\bar{C}_B$ < 0.5 the threshold speed has been increased significantly be-

yond that for $\bar{K}_B = 0.1$. By increasing the support stiffness to $\bar{K}_B = 1.0$ with $\delta m = 0.1$, the optimum damping values remain at approximately $\bar{C}_B \sim 0.5$–1.0 and the lightly damped support threshold speed is slightly better than in Fig. 8, but still below the rigid support onset speed (see Fig. 10*(b)*). The stability maps shown as Figs. 10*(c)* and 10*(d)* clearly indicate that an increase of support mass greatly reduces the maximum onset speed whereas a lighter support system can be designed to increase the threshold speed to extremely high values for support damping values between $\bar{C}_B = 0.01$ and 1.0. The overdamped condition ($\bar{C}_B > 10$) remains at about the same threshold speed for all the variations considered in this series of stability maps.

The importance of proper design of support structures is further illustrated in Fig. 11*(a)* where, for the specific condition of $\bar{K}_B = 1.0$ and $\delta m = 0.1$, the optimum support damping is indicated to be $\bar{C}_B \sim 1.0$. This value of damping would be ideal for both the lightly loaded and heavily loaded condition. Fig. 11*(b)* indicates that by reducing $\bar{K}_B$ to 0.1 with $\delta m = 0.01$ the range of acceptable support damping is greatly increased. However, for the heavily loaded system ($\bar{W} > 100$), the optimum damping must be properly chosen to insure the greatest stable operating speed range.

These stability maps indicate that the plain journal bearing can be designed with a flexible damped support such that the stable operating speed range is greatly extended beyond the rigid support threshold speed. Equally important, the analysis indicates that improper support design could possibly lower the threshold speed below that which would be obtained for rigid supports.

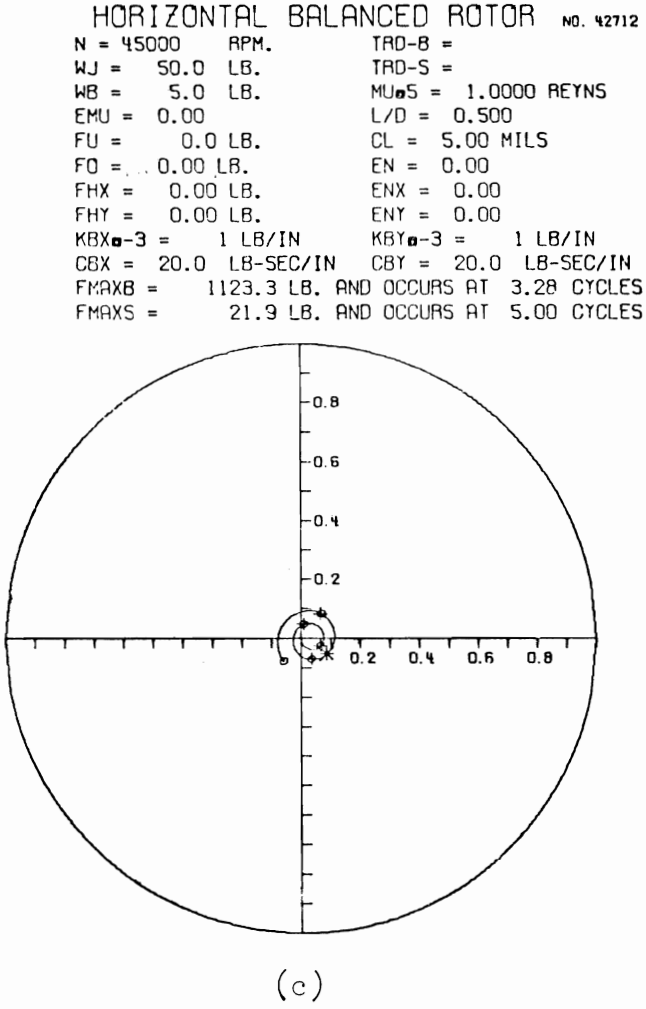

Fig. 9*(c)* Rotor relative motion for five cycles showing instability (N = 45,000 rpm, ω_s = 17)

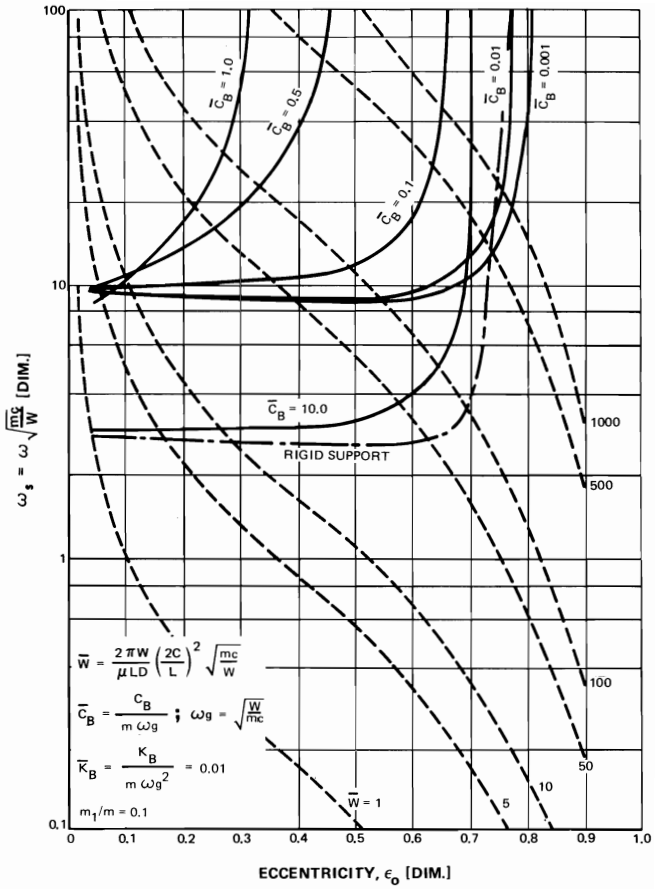

Fig. 10*(a)* Stability map for the damped, flexible support rotor on short journal bearings ($\bar{K}_B = 0.01$, $m_1/m = 0.1$)

4.2 TRANSIENT RESPONSE ANALYSIS. Stability maps such as the ones presented in the previous section of this paper are of great value due to the amount of useful information contained on a single plot. The analysis of time-transient response of rotor systems cannot be presented in such a compact form. However, the amount of design information obtained from an actual time-transient response analysis for a specific rotor system easily justifies the effort required to produce and interpret the results.

The technique for calculation of the transient response has been discussed in detail in several references [11, 22]. The initial value problem requires only that the displacements and velocities of the rotor system be given at a specific initial starting time. From this information the nonlinear fluid-film forces may be calculated (as shown in equation (3)) and any other forces specified as a function of time, displacement, and velocity may also be included in the simulation.

The equations of motion in dimensionless form are expressed as follows:

$$\ddot{X}_1 + \ddot{X}_j = \frac{F_x(X, Y, \dot{X}, \dot{Y})_j}{mc\omega_j^2} + E_\mu \cos(T) + \frac{1}{2mc\omega_j^2} f_x(l) - \frac{C_s}{2m\omega_j}(\dot{X}_1 + \dot{X}_j) \quad (24a)$$

$$\ddot{Y}_1 + \ddot{Y}_j = \frac{F_y(X, Y, \dot{X}, \dot{Y})_j}{mc\omega_j^2} + E_\mu \sin(T) + \frac{1}{2mc\omega_j^2} f_y(l) - \frac{g}{c\omega_j^2} - \frac{C_s}{2m\omega_j}(\dot{Y}_1 + \dot{Y}_j) \quad (24b)$$

$$\delta m\, \ddot{X}_1 = \frac{1}{mc\omega_j^2}(F_{Px} - F_x(X, Y, \dot{X}, \dot{Y})_j) - \left[\frac{K_{1xx}}{m\omega_j^2} X_1\right.$$

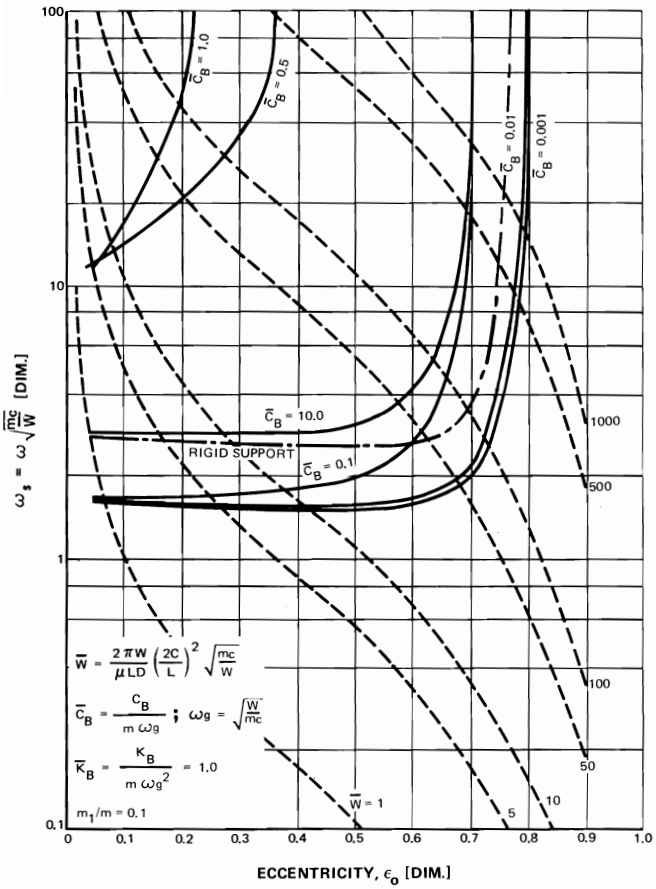

Fig. 10*(b)* Stability map for the damped, flexible support rotor on short journal bearings ($\bar{K}_B$ = 1.0, m_1/m = 0.1)

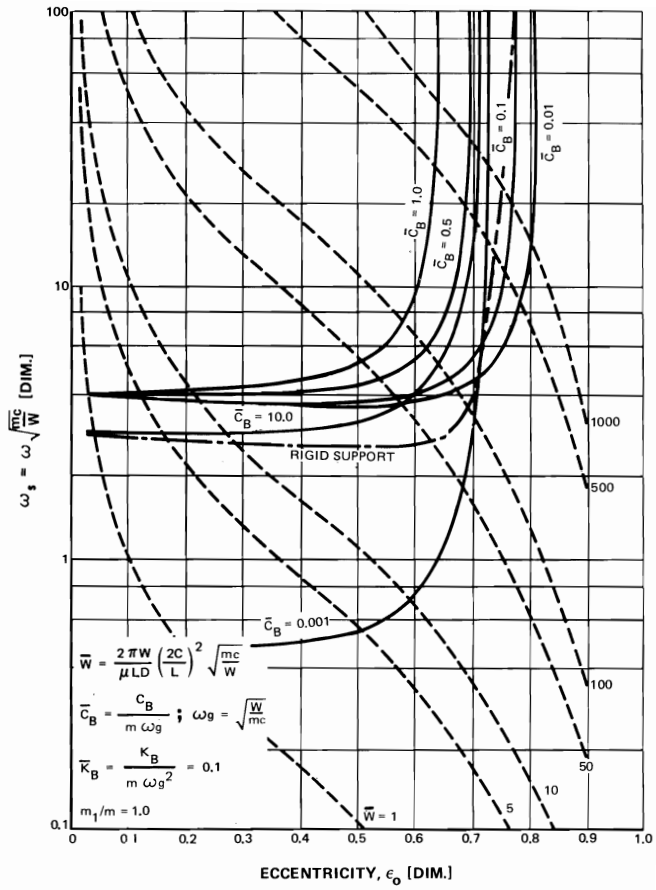

Fig. 10*(c)* Stability map for the damped, flexible support rotor on short journal bearings ($\bar{K}_B$ = 0.1, m_1/m = 1.0)

$$+ \frac{K_{1xy}}{m\omega_j^2} Y_1 + \frac{C_{1xx}}{m\omega_j} \dot{X}_1 + \frac{C_{1xy}}{m\omega_j} \dot{Y}_1] \quad (24c)$$

$$\delta m \ddot{Y}_1 = \frac{1}{mc\omega_j^2}(F_{py} - F_y(X, Y, \dot{X}, \dot{Y})_j) - [\frac{K_{1yy}}{m\omega_j^2} Y_1 + \frac{C_{1xx}}{m\omega_j^2} X_1 + \frac{C_{1yy}}{m\omega_j} \dot{Y}_1 + \frac{C_{1yx}}{m\omega_j} \dot{X}_1] - \delta m \frac{g}{c\omega_j^2} \quad (24d)$$

where the equation for $\bar{F}(x,y,\dot{x},\dot{y})$ is given by equation 4.

The addition of a flexible, damped support system has been shown in Example 2 to greatly increase the threshold speed if the support is properly designed. There are instances where the support can be poorly designed and produce no harmful results as long as the rotor speed remains below the stability threshold. However, the bearing and support loading will in most all cases be higher than if the support system were properly designed.

It was seen in the transient orbits shown in Fig. 9 that by proper design of the support system for the rotor of Example 1, the stability threshold could be increased from 6500 rpm to over 31,500 rpm. The transient orbit analysis for the nonlinear system also shows that even well above the stability threshold at a speed of 45,000 rpm, the unstable motion increases with a small growth rate. The design conditions for the support system is given by Example 2 with $\bar{K}_b$ = 0.1.

$$\bar{C}_b = 0.556 \text{ and } \delta_m = 0.1$$

It is important to note that it is extremely difficult to determine the optimum damper support system by use of the time-transient program for the integration of the nonlinear equations of motion. In the initial phases of the investigation of the influence of the damper support system on journal stability, the time-transient program was developed and run prior to the development of the linearized stability analysis. Numerous runs were made with the time transient program to incorporate various damper combination to stabilize the rotor orbits as shown in Figs. 6 and 7 at 10,500 rpm with little success. It was only after the linearized stability analysis was developed that the successful damper combination as shown in Fig. 9 was arrived at.

Example 3—Off Tuned Support System. Consider the system of Fig. 12 in which the support stiffness is assumed to be K_b = 10,000 lb/in. and the support damping is C_b = 200 lb s/in.

$$\bar{K}_b = \frac{10{,}000 \text{ lb/in.}}{M\omega g^2} = 1.0, \ \bar{C}_b = \frac{200}{M\omega g^2} = 5.56$$

The stability chart corresponding to the damper parameters of $\bar{K}_b$ = 1.0 and δ_m = 0.1 is given by Fig. 10*(b)*. At a speed of N = 6500 rpm as shown in Fig. 12*(a)* the rotor shows a very stable elliptic orbit about the equilibrium position of ϵ_0 = 0.211. It is of interest to note that for this level of unbalance, the synchronous elliptic journal orbit can be predicted accurately by use of the linearized bearing coefficients. Fig. 12*(b)* represents the absolute motion of the support system. The support system has a static vertical displacement of 0.0055 in. due to its 50-lb weight of the journal and 5-lb weight of the support housing acting on the 10,000 lb/in. support spring rate. The dimensionless vertical equilibrium position of the support system is $Y = -0.0055/C = -1.1$. The absolute motion of the support housing is a circular synchronous orbit of dimensionless radius 0.2 caused by the imbalance dim. eccentricity of EMU = 0.20.

From Fig. 10*(b)*, the value of $\bar{C}_b$ = 5.56 represents excessive damping and the stability curve will be close to the $\bar{C}_B$ = 10 curve. Although the support system damping is excessive, the stability threshold is still increased by about 25 percent over the rigid sup-

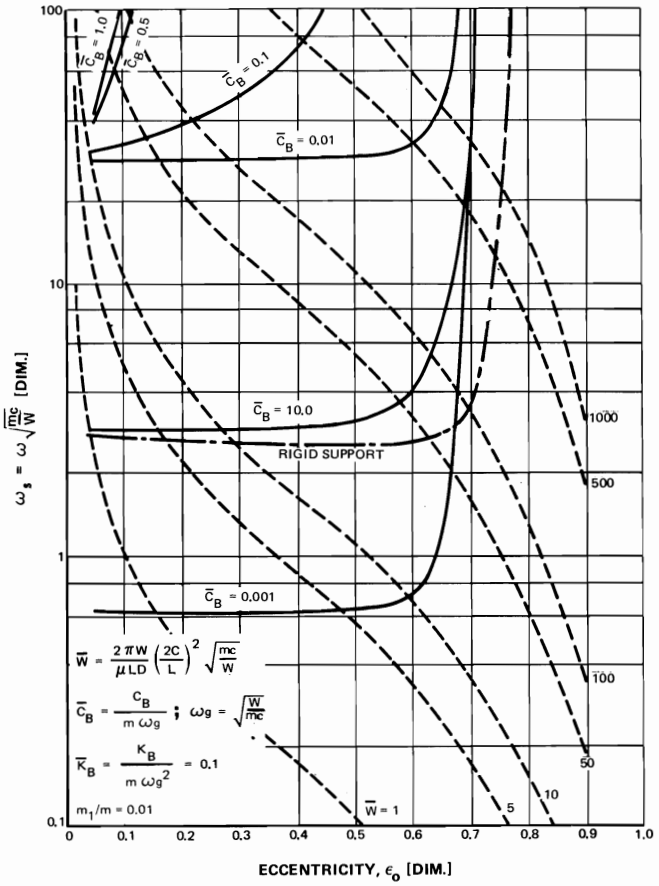

Fig. 10*(d)* Stability map for the damped, flexible support rotor on short journal bearings ($\bar{K}_B$ = 0.1, m_1/m = 0.01)

port condition.

The system stability would only be reduced below the rigid support condition in the case that the support damping drops below $\bar{C}_B$ = 0.1. In this example, this would be equivalent to a reduction in the damping from 200 lb s/in. to less than 4 lb s/in. Therefore we see that if the support system losses its damping, the stability threshold is reduced below the rigid support condition. There have been instances reported where rotating machinery would suffer from violent bearing instability when the rotor casing was not firmly anchored down. Upon securely bolting down the casing, the whirl instability would disappear. This is similar to the situation of the introduction of support flexibility without any accompanying support damping which is required for stabilization.

If the rotor speed is increased from 6500 rpm to 10,500 rpm, the system is no longer stable as shown in Fig. 14. Fig. 14*(a)* shows that the journal has a substantial fractional frequency whirl orbit. It is apparent from the examination of the journal and support orbits that the system is operating well above the stability threshold. The orbit of the support housing has increased over 2-½ times the support housing motion at 6500 rpm. In an attempt to reduce the whirl orbit experienced at 10,500 rpm, a case was run with the damping increased to 400 lb-s/in. The resulting whirl orbit was much worse than the orbit obtained with 200 lb-s/in. damping in the system. Upon the development of the stability threshold map as shown in Fig. 10, it is readily apparent that in order to increase the stability for this system, the damping should have been reduced rather than increased. The optimum damping for $\bar{K}_B$ = 1.0 lies between $\bar{C}_B$ = 0.5 and 1.0 which represents damping values of 18–36 lb-s/in.

Although the damping in Fig. 13 is excessive, and the rotor is unstable at 10,500 rpm, the resulting limit cycle will still be smaller than the motion obtained with the rigidly supported journal as shown in Figs. 6 and 7.

The properly designed support system cannot only greatly improve the threshold of stability of the hydrodynamic journal bearing, but it can result in a substantial attenuation of the forces transmitted through the support structure due to imbalance. Fig. 14 represents the journal at 10,500 rpm with the optimum support damper as given in Example 2 with $\bar{K}_B$ = 0.10, $\bar{C}_B$ = 0.556 and δ_m = 0.1.

One of the important questions besides the stability threshold characteristics is what will be the size of the rotor orbit and the journal and bearing forces transmitted through the system. At 10,500 rpm, the dimensionless imbalance eccentricity of *EMU* =

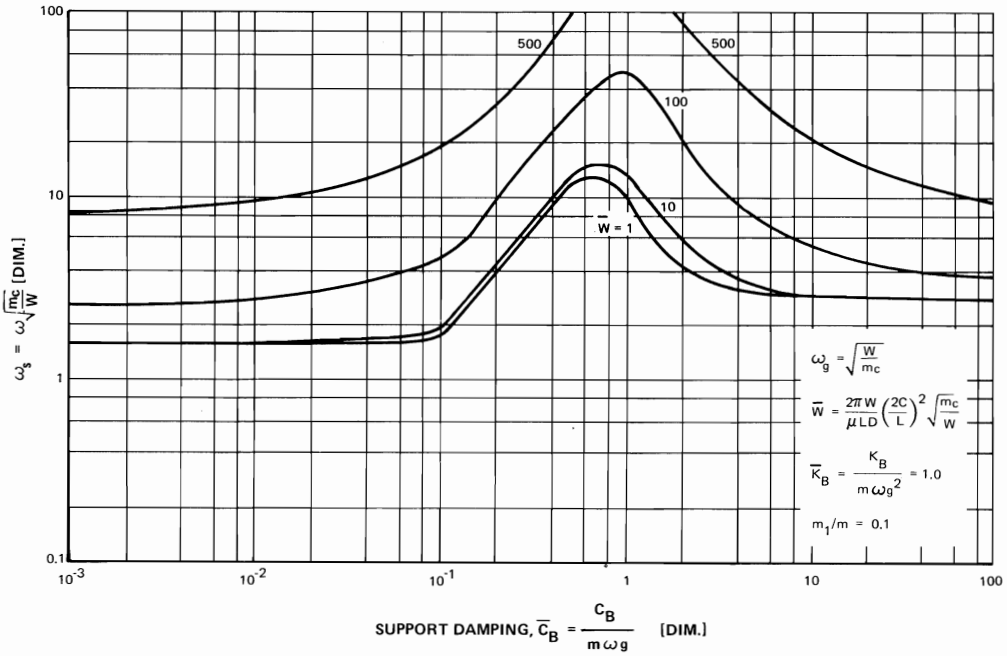

Fig. 11*(a)* Stability map showing the threshold speed versus support damping ($\bar{K}_B$ = 1.0, m_1/m = 0.1)

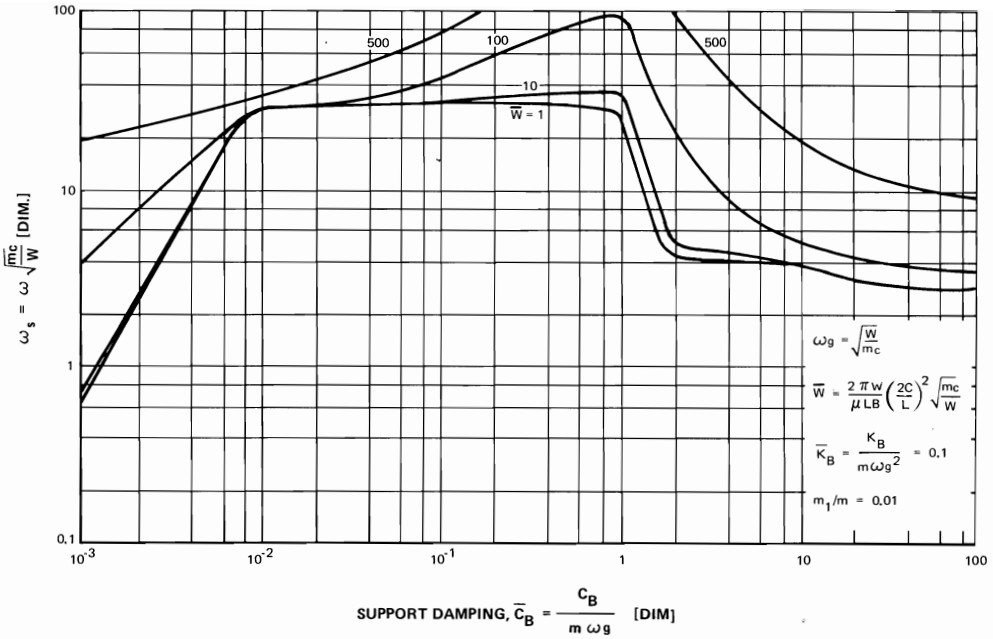

Fig. 11*(b)* **Stability map for reduced support stiffness and damping indicating a larger region of stable operation ($K_B = 0.1$, $m_1/m = 0.01$)**

HORIZONTAL UNBALANCED ROTOR

NO.111894

N = 6500 RPM.	
WJ = 50.0 LB.	MU*S = 1.0000 REYNS
WB = 5.0 LB.	L/D = 0.500
EMU = 0.20	CL = 5.00 MILS
FO = 0.00 LB.	EN = 0.00
FHX = 0.00 LB.	ENX = 0.00
FHY = 0.00 LB.	ENY = 0.00
KBX*-3 = 10 LB/IN	KBY*-3 = 10 LB/IN
CBX = 200.0 LB-SEC/IN	CBY = 200.0 LB-SEC/IN

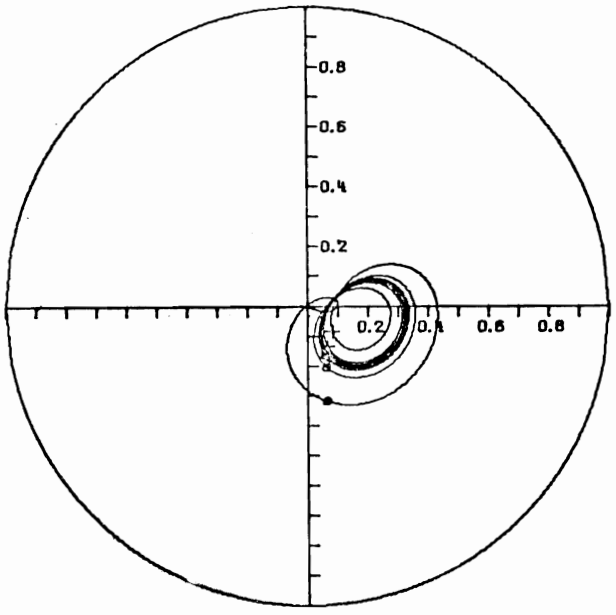

(a)

Fig. 12*(a)* **Journal relative motion on flexible supports showing steady-state elliptic orbit ($N = 6500$ rpm, $\omega_s = 2.45$)**

HORIZONTAL UNBALANCED ROTOR

NO.111894

N = 6500 RPM.	
WJ = 50.0 LB.	MU*S = 1.0000 REYNS
WB = 5.0 LB.	L/D = 0.500
EMU = 0.20	CL = 5.00 MILS
FO = 0.00 LB.	EN = 0.00
FHX = 0.00 LB.	ENX = 0.00
FHY = 0.00 LB.	ENY = 0.00
KBX*-3 = 10 LB/IN	KBY*-3 = 10 LB/IN
CBX = 200.0 LB-SEC/IN	CBY = 200.0 LB-SEC/IN

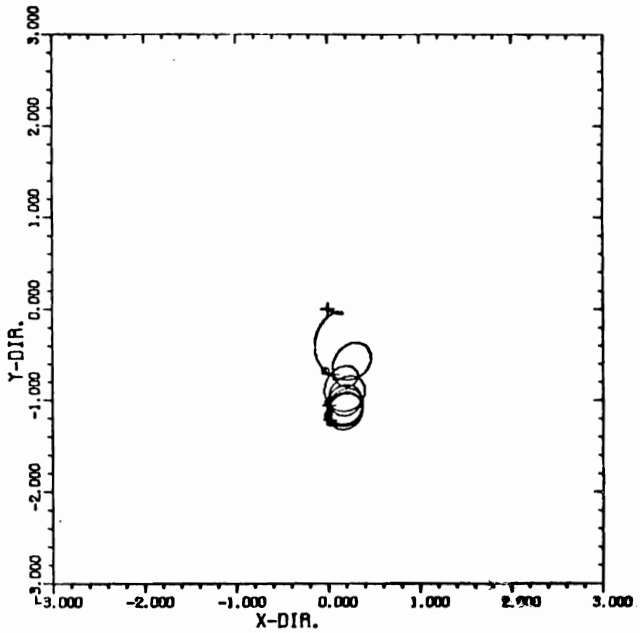

(b)

Fig. 12*(b)* **Support transient motion ($N = 6500$ rpm)**

0.2 represents a rotating load of 155.6 lb. The maximum force transmitted through the bearing is 249 lb which represents a dynamic transmissibility through the bearing of *TRD-B* = 1.591. Normally a dynamic transmissibility in excess of one is considered undesirable as this indicates that the rotating imbalance force has been amplified. That is, more force is being transmitted through the bearing than would be if the bearing were perfectly rigid. However, with the damper support, only 33.6 lb. force is transmitted from the support system to the base. Therefore the dynamic transmissibility that is felt by the surrounding foundation has been greatly attenuated since *TRD-S* = 0.214. Hence it is seen that a well designed damper support can cause a great reduction in the forces transmitted through the foundation. In the extensive study conducted on the nonlinear transient analysis of journal bearings [22], it is observed that with imbalance the journal dynamic transmissibility was usually greater than one. Therefore it appears that the damper support can reduce the dynamic transmissibility which should promote smoother turbomachinery operation.

5. Conclusions

The following observations and conclusions may be stated concerning the results that have been presented in this paper.

1 The use of a flexible damped support system may greatly increase the stability threshold of the plain journal bearing.

2 Lightly loaded rotors with low load parameters ($\bar{W} = 1$) are more difficult to stabilize than heavily loaded rotors in which the load parameter $\bar{W}$ is greater than 100.

3 For lightly loaded rotors, the optimum damper support may increase the stability threshold over four times of that obtainable with the rigidly supported plain journal bearing. The maximum stability threshold in RPM with an optimum damper support for a lightly loaded rotor is given approximately by

$$N_s = 100\sqrt{\frac{W}{mc}} \tag{25}$$

4 The damper support performs most effectively when the support housing weight is kept less than the rotor weight. If δ_m exceeds unity, then the damper support system will provide little increase in stability above the rigid support values.

5 If the bearing support stiffness $\bar{K}_B$ is excessive (>5) then the high stiffness will prevent the damper support from improving the journal stability. The preferential support stiffness design value should be $\bar{K}_b < 1$. Hence the support stiffness should be designed such that

$$K_b \leq M\omega g^2 = m\left(\frac{W}{mc}\right) = \frac{W}{C} \tag{26}$$

For example, with a 50-lb journaland a 0.005-in. radial clearance bearing, the support stiffness should be 10,000 lb/in. or less.

6 It may be difficult to improve the stability of high speed light weight rotors with a damper support system because of the low support flexibility required.

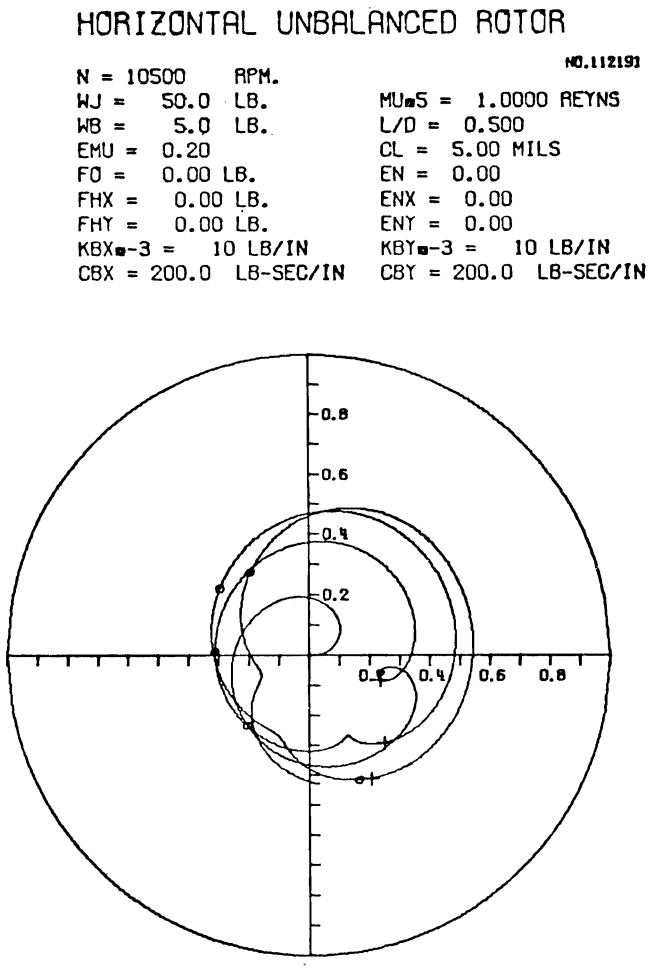

(a)

Fig. 13(*a*) Journal transient response for an overdamped support (N = 10,500 rpm, $E\mu$ = 0.2)

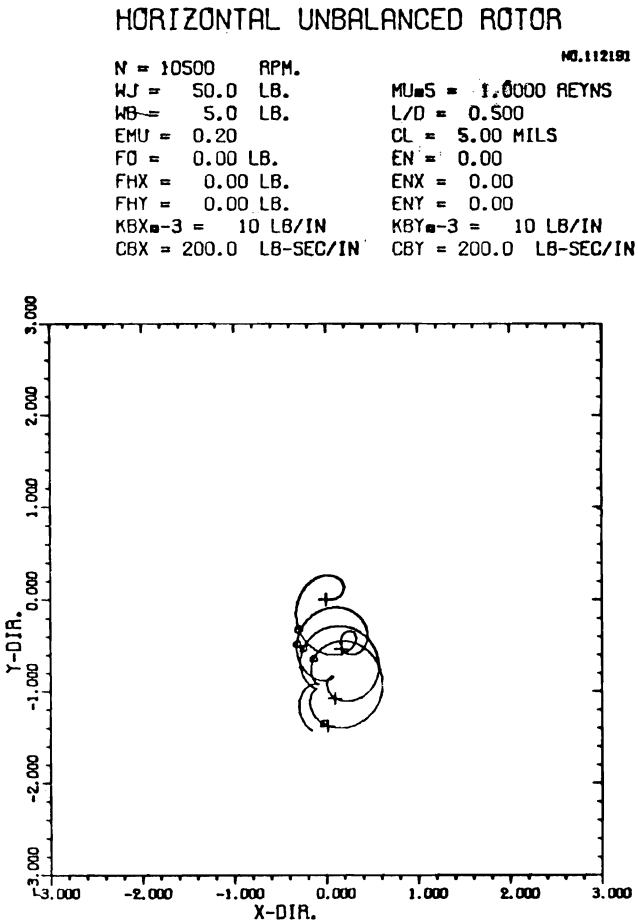

(b)

Fig. 13(*b*) Support response ($\bar{K}_B$ = 1.0, $\bar{C}_B$ = 5.56)

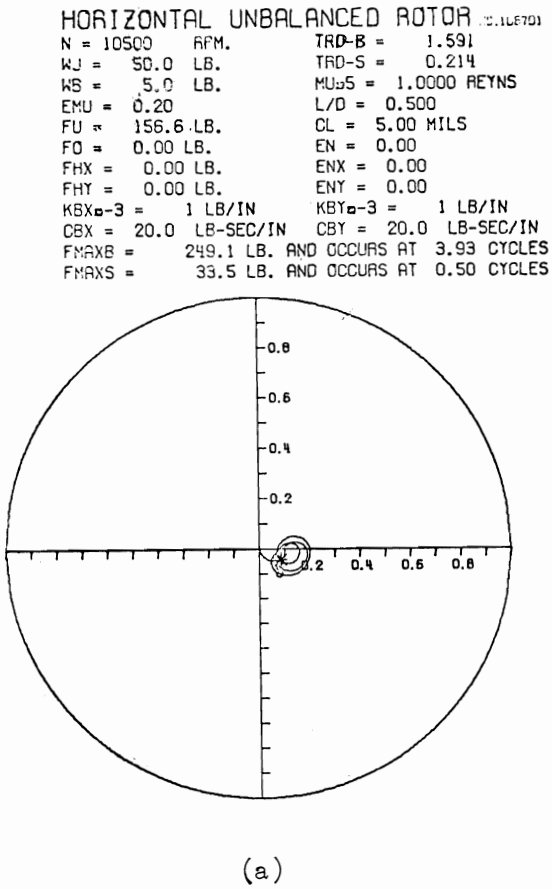

(a)

Fig. 14(a) Journal response for improved support characteristics (N = 10,500 rpm, $E\mu = 0.2$)

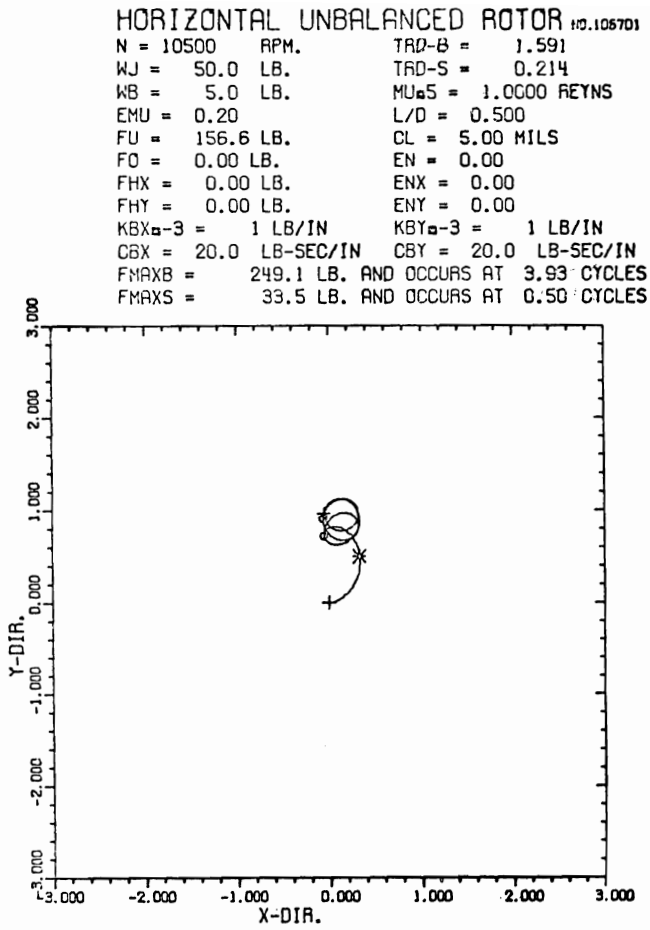

(b)

Fig. 14(b) Support system response for five cycles ($\bar{K}_B = 0.1$, $\bar{C}_B = 0.556$)

7 There is an optimum support damping that should be incorporated with the flexible support. If the support damping $\bar{C}_B$ exceeds 10, then there will be little beneficial effects from the damper in promoting stability. The optimum design range of $\bar{C}_B$ should be between approximately 0.5–1.0. Hence the actual damping should be designed as

$$C_B = (0.5 - 1.0)\, M\omega g = (0.5 - 1.0)\sqrt{\frac{MW}{C}} \quad (27)$$

For example, the optimum support damping for a 50-lb horizontal gravity loaded rotor with a 5-mil bearing clearance would be between 18–36 lb-s/in.

8 If the support damping becomes too light ($\bar{C}_b < 0.1$) then the support flexibility will cause a reduction of the stability threshold below the rigid support values. Therefore, the loss of damper fluid in a squeeze film damper system operating well above the rigid support stability threshold could result in a violent whirl motion which is more severe than the whirl orbit of the rigidly mounted bearing.

9 The nonlinear time-transient method of analysis may be used to investigate the journal limit cycles on rigid or damped supports. For stable operation with low values of imbalance ($EMU <$ 0.2) then linearized bearing theory may be used to adequately predict the rotor synchronous whirl orbits. However, for unstable operation or large levels of imbalance, then the nonlinear time-transient method must be used to determine the journal limit cycles and forces transmitted.

10 High values of imbalance can cause the journal motion to change from nonsynchronous to synchronous in both the horizontal and vertical rotors. However, the introduction of deliberate imbalance in a journal in order to stabilize it is not recommended because of the forces transmitted.

11 The vertical balanced unloaded journal is inherently unstable in a rigid or a damped flexible support. However, the limit cycle motion is considerably smaller with the damper support.

12 Even if the support stiffness and damping characteristics are excessive, the resulting whirl orbits obtained above the stability threshold will be smaller than that obtained with the rigid mounted journal bearing.

13 The nonlinear analysis indicates that with a well designed support system, the threshold of stability may be considerably exceeded with only small limit cycle whirl motion.

14 It is difficult to operate the journal bearing on rigid supports with imbalance values $EMU > 0.2$ and keep the dynamic transmissibility below unity.

15 With a well designed damper support, the dynamic transmissibility from the support to the foundation can be kept well below unity even for large rotor imbalances. Therefore damper supports should promote smoother and quieter machine operation due to the suppression of oil whirl and the attenuation of the rotating unbalance forces.

Acknowledgment

This research work was supported by NASA Lewis Research Center, Cleveland, Ohio, Grant No. NGR 47-005-050, Industrial Grant 543-H, University of Virginia. The authors wish to express their appreciation to Mr. Robert Cunningham, Project Monitor and Mr. William J. Anderson, Director Bearings Branch, for their

support and constant encouragement of this work.

References

1 Newkirk, B. L., "Shaft Whipping," *Gen. Elec. Rev.,* Vol. 27, 1924, p. 169.

2 Newkirk, B. L., and Taylor, H. D., "Shaft Whipping Due to Oil Action in Journal Bearings," *Gen. Elec. Rev.,* Vol. 28, 1925, pp. 985–988.

3 Robertson, D., "Whirling of a Journal in a Sleeve Bearing," *Phil. Mag.,* Series 7, Vol. 15, No. 66, Jan. 1933.

4 Hagg, A. C., "The Influence of Oil Film Journal Bearings on the Stability of Rotating Machines," *Journal of Applied Mechanics,* TRANS. ASME, Vol. 68, 1946, p. 211.

5 Orbeck, F., "Theory of Oil Whip for Vertical Rotors Supported by Plain Journal Bearings," TRANS. ASME, Oct. 1958, pp. 1497–1502.

6 Pinkus, O., "Experimental Investigation of Resonant Whip," TRANS. ASME, Vol. 78, 1956, pp. 975–983.

7 Poritsky, H., "Contribution to the Theory of Oil Whip," TRANS. ASME, Aug. 1953, pp. 1153–1161.

8 Hagg, A. C., and Warner, P. C., "Oil Whip of Flexible Rotors," TRANS. ASME, Vol. 75, Oct. 1953, pp. 1339–1344.

9 Gunter, E. J., "Dynamic Stability of Rotor-Bearing Systems," NASA SP-113, 1966.

10 Hori, Y., "Theory of Oil Whip," *Journal of Applied Mechanics,* Vol. 26, TRANS. ASME, Series E, Vol. 81, 1959, p. 189.

11 Badgley, R. H., "Turborotor Instability—Dynamic Unbalance, Gyroscopic, and Variable-Speed Effects with Finite-Length, Cavitated, Fluid-Film Bearings," PhD dissertation, Cornell University, Ithaca, N. Y., June 1967.

12 Lund, J. W., "The Stability of an Elastic Rotor in Journal Bearings With Flexible, Damped Supports," *Journal of Applied Mechanics,* TRANS. ASME, Series E, Vol. 87, No. 4, Dec. 1965, pp. 911–920.

13 Günter, E. J., "The Influence of Flexibility Mounted Rolling Element Bearings on Rotor Response, Part 1: Linear Analysis, *"Journal of Lubrication Technology,* TRANS. ASME, Jan. 1970, pp. 59–75.

14 Ruhl, R. L., "Dynamics of Distributed Parameter Rotor Systems: Transfer Matrix and Finite," PhD dissertation, Cornell University, Ithaca, N. Y., Jan. 1970.

15 Lund, J. W., "Stability and Damped Critical Speeds of a Flexible Rotor in Fluid-Film Bearings," JOURNAL OF ENGINEERING FOR INDUSTRY, TRANS. ASME, Series B, Vol. 96, No. 2, May 1974, pp. 509–517.

16 De Choudhury, P., "Dynamic Stability of Flexible Rotor-Bearing Systems," PhD dissertation, University of Virginia, Charlottesville, Va., June 1971.

17 Kirk, R. G., and Gunter, E. J., "Nonlinear Transient Analysis of Multi-Mass Flexible Rotors—Theory and Applications," NASA CR-2300, Sept. 1973.

18 Newkirk, B. L., "Varieties of Shaft Disturbances Due to Fluid Films in Journal Bearings," TRANS. ASME, Vol. 78,1956, p. 985.

19 Ocvirk, F. W., "Short-Bearing Approximation for Full Journal Bearings," NACA TN 2808, 1952.

20 Badgley, R. H., and Booker, J. F., "Turborotor Instability: Effect of Initial Transient on Plane Motion," *Journal of Lubrication Technology,* Trans. ASME, Oct. 1969, pp. 625–633.

21 Reddi, M. M., and Trumpler, P. R., "Stability of the High-Speed Journal Bearing Under Steady Load—1 The Incompressible Film," JOURNAL OF ENGINEERING FOR INDUSTRY, TRANS. ASME, Series B, Vol. 84, 1962, pp. 351–358.

22 Kirk, R. G., and Gunter, E. J., "Transient Journal Bearing Analysis," NASA CR-1549, Washington, D. C., June 1970.

23 Beckett, R., and Hurt, J., *Numerical Calculations and Algorithms,* McGraw-Hill, New York, 1967, p 70.

24 Kirk, R. G., "Nonlinear Transient Analysis of Mult-Mass Flexible Rotors," PhD dissertation, University of Virginia, Charlottesville, Va., June 1972.

25 Lund, J. W., "Self-Excited, Stationary Whirl Orbits of a Journal in a Sleeve Bearing," PhD dissertation, Rensselaer Polytechnic Institute, Troy, N.Y., April 1966.

26 Poritsky, H., "Contributions to the Theory of Oil Whip," TRANS. ASME, Vol. 75, 1953, pp. 1153–1161.

27 Holmes, R., "The Vibration of a Rigid Rotor on Short Journal Bearings,,: *Journal of Mechanical Engineering Science,* Vol. 2, No. 4, 1960, p. 337.

Printed in U. S. A.